ELSEVIER

Journal of Volcanology and Geothermal Research 110 (2001) 27–55

Journal of volcanology and geothermal research

www.elsevier.com/locate/jvolgeores

Analytical/numerical modeling of komatiite lava emplacement and thermal erosion at Perseverance, Western Australia

David A. Williams[a,b,*], Ross C. Kerr[c], C. Michael Lesher[b,d], Stephen J. Barnes[e]

[a]*Department of Geological Sciences, Arizona State University, Box 871404, Tempe, AZ, 85287-1404, USA*
[b]*formerly Department of Geological Sciences, University of Alabama, Tuscaloosa, AL, 35487-0338, USA*
[c]*Research School of Earth Sciences, The Australian National University, Canberra, ACT, 0200, Australia*
[d]*Mineral Exploration Research Centre and Department of Earth Sciences, Laurentian University, Sudbury, Ontario, P3E 6B5, Canada*
[e]*CSIRO Division of Exploration and Mining, Perth, Western Australia, 6014, Australia*

Received 13 April 2000; revised 24 January 2001; accepted 24 January 2001

Abstract

We have applied a thermal–fluid dynamic-geochemical model to investigate the emplacement and erosional potential of Archean komatiite flows at Perseverance, Western Australia. Perseverance has been proposed as a site of large-scale thermal erosion by large-volume komatiite eruption(s), resulting in a 100–150-m-deep lava channel containing one of the world's largest komatiite-hosted Fe–Ni–Cu–(PGE) sulfide deposits. Using constraints based on field, theoretical, and geochemical data, we have modeled the emplacement of a range of flow thicknesses over felsic tuffaceous substrates with various degrees of consolidation and water contents. Thermo-mechanical erosion becomes more effective for substrates that are increasingly unconsolidated and water rich. For thermo-mechanical erosion to be responsible for the formation of the ~100-m-deep, concave Perseverance embayment and the highly-contaminated (~10–20%) Perseverance komatiites, the most likely scenarios require emplacement of thick (e.g. ≥10–30 m), turbulent, channelized liquidus or superheated komatiite lavas over a welded or unconsolidated submarine tuff. Flow distances must have been long (tens to hundreds of kilometers) and flow volumes must have been very high (hundreds to thousands of km^3). Lava channels and tubes >110 km long have not been observed on Earth, but are consistent with those formed by low-viscosity lavas on Venus, the Moon, Mars and Io. Flow volumes are consistent with those in continental flood basalt eruptions and oceanic plateau Large Igneous Provinces, and may represent the initial outpourings of komatiite lavas from Archean mantle plume activity.

Keywords: numerical modelling; lava emplacement; komatiite; thermal erosion; Perseverance

1. Introduction

One of the remarkable features inferred from the compositions of Precambrian komatiite lavas is their capability for turbulent flow and thermal erosion of substrate when emplaced as channelized flows (Huppert et al., 1984; Lesher et al., 1984; Huppert and Sparks, 1985a; Huppert, 1989). Thermal erosion and assimilation of sulfur-rich substrates are considered to be necessary elements in the formation of komatiite-associated Fe–Ni–Cu–(PGE) sulfide deposits (see reviews by Lesher, 1989; Naldrett, 1989; and paper by Lesher and Campbell, 1993). The recent work of Williams et al. (1998), which

* Corresponding author. Tel.: +1-480-965-7029; fax: +1-480-965-8102.

E-mail addresses: dwilliams@dione.la.asu.edu (D.A. Williams), ross.kerr@anu.edu.au (R.C. Kerr), lesher@sympatico.ca (C.M. Lesher), barnes.s@per.dem.csiro.au (S.J. Barnes).

0377-0273/01/$ - see front matter
PII: S0377-0273(01)00206-2

has built on the landmark study of komatiite flow and thermal erosion by Huppert and Sparks (1985a), has discussed some of the complexities in modeling komatiite emplacement and thermal erosion, including the much greater potential for thermo-mechanical erosion of unconsolidated, water-rich sediments than consolidated rocks. In this paper, we turn our attention to another site where thermal erosion by komatiite flows has been proposed: Perseverance, Western Australia (Barnes et al., 1988a). We begin first with a brief review of the physical and geochemical nature of komatiites which supports their potential for turbulent flow and thermal erosion, and we follow with a review of the geology of the Perseverance Ultramafic Complex from previous and recent studies. Next, we review the elements of our analytical/numerical model for komatiitic lava emplacement and thermal erosion, including required assumptions and limitations, and then we discuss modifications made to the model to investigate the nature of komatiite emplacement at Perseverance. Finally, we report our model results and attempt to place them in the broader context of Archean and planetary volcanism.

2. Background

2.1. Komatiites and thermal erosion

Komatiites are ultramafic volcanic rocks, typically characterized by high MgO contents and spinifex or cumulate textures, which are almost completely restricted to Precambrian terrains (Arndt and Nisbet, 1982). Although they may be metamorphosed, original igneous textures and parts of their igneous mineralogy are commonly preserved (Viljoen and Viljoen, 1969a,b; Ross and Hopkins, 1975; Arndt et al., 1977; Hill et al., 1990, 1995). Petrological studies on well preserved samples suggest that Archean komatiite liquids (Table 1) were low in SiO_2 ($\leq$45–47%) and high in MgO ($\geq$18–32%), and, thus, are inferred to have had high liquidus temperatures (~1360–1640°C), low dynamic viscosities (~0.1–2 Pa s: Nisbet, 1982), high densities (>2800 kg/m^3), and to have erupted as very voluminous, highly mobile, locally channelized flows (Lesher et al., 1984). Because hot, turbulent fluids lose heat rapidly by convection, which is a more efficient mechanism of heat transfer than conduction, Huppert and Sparks (1985a) showed that channelized komatiite lava flows should have had a great potential for thermal erosion of massive, consolidated felsic and mafic substrates (see also Huppert, 1989, who showed that the initial chilled margin at the base of turbulent flows will grow to a thickness of less than 1 cm and will be remelted in a time of the order of 30 s).

Although a broad definition of thermal erosion may include both: (a) thermal ablation (melting) of substrate, and (b) physical degradation (mechanical erosion) with plucking and removal of unconsolidated or loosened material by the force of the moving flow, Huppert and Sparks (1985a) discussed only ablation in their work. They suggested that thermal erosion incised deep (~tens of meters) reentrant-shaped lava channels into a flat basaltic ocean floor at Kambalda, Western Australia, and that erosion of interflow S-rich sedimentary material led to the formation of dense sulfide melts that accumulated at the base of the Kambalda embayments. Their modeling, however, is at odds with field observations at Kambalda (Lesher, 1983; Lesher et al., 1984; Lesher, 1989), which suggest that pre-existing topography or lava channels existed in the basaltic sea floor, and that only minor (<1 m) basalt erosion occurred. This minor basalt erosion is thought to have been caused by hot sulfide melts rather than komatiite lavas (Lesher et al., 1984; Groves et al., 1986; Evans et al., 1989). This hypothesis was disputed by Arndt (1986), but the criticism was based on the invalid assumption that the entire sulfide layer acted as a thermal boundary layer. Subsequent isotopic and geochemical studies at Kambalda (Arndt and Jenner, 1986; McNaughton et al., 1988; Frost and Groves, 1989; Lesher and Arndt, 1995) support *local* erosion of a felsic contaminant (presumably the thin, ~1–5-m-thick layers of S-rich, unconsolidated interflow sediments), but not necessarily a mafic contaminant. Since the work of Huppert and Sparks, additional sites of komatiite-associated thermal erosion have been proposed, including Perseverance, Western Australia (Barnes et al., 1988a, 1995), Katinniq and several other exposures in the Cape Smith Belt, New Québec (Gillies and Lesher, 1992; Lesher et al., 2001a), Mickel, Abitibi greenstone belt, Canada (Davis et al., 1993), and Forrestania, Western Australia (Perring et al., 1995). Thermal erosion has been inferred to occur in several terrestrial lava tubes

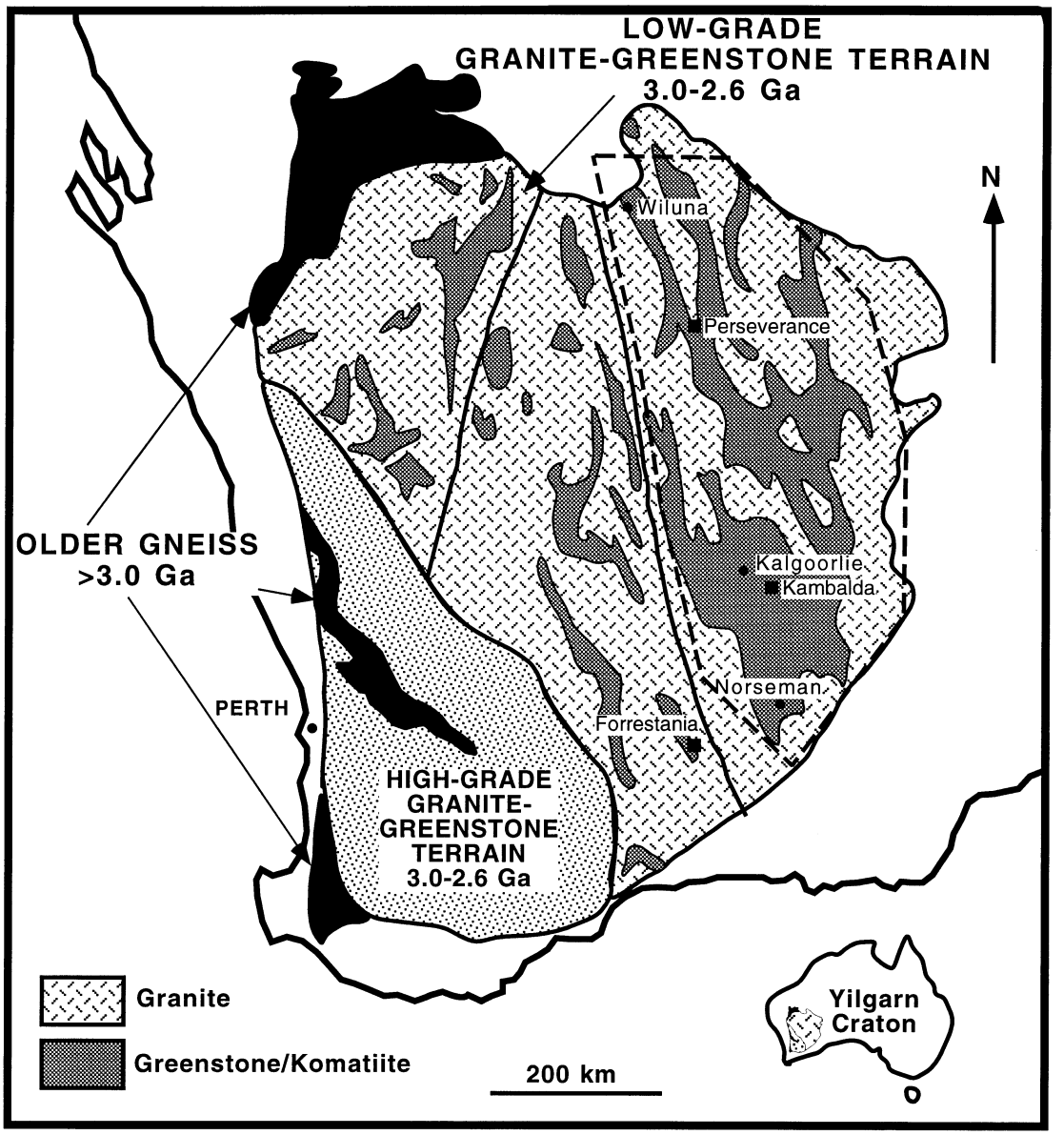

Fig. 1. Geologic map of the Yilgarn Craton, Western Australia. Dashed line indicates the Norseman–Wiluna greenstone belt. Black squares mark sites of proposed thermal erosion channels. After Myers (1988); Gee et al. (1981).

(see review in Greeley et al., 1998). Recently, thermal erosion has been measured directly in laminarly-flowing Hawaiian lava tubes, with rates ~10 cm/day (Swanson, 1973; Kauahikaua et al., 1998) that have been quantitatively explained by Kerr (2001). Thermal erosion was also proposed as a possible mode of origin of the lunar sinuous rilles and some Martian volcanic channels (Hulme, 1973; Carr, 1974), and it became a subject of interest in the 1990s as a possible cause of long lava channels on Venus (Head et al., 1991; Baker et al., 1992). Recently, Galileo spacecraft, Hubble Space Telescope, and Earth-based telescopic observations have detected high-temperature, possibly ultramafic silicate eruptions on Jupiter's

Table 1
Inferred liquid compositions and physical properties for several komatiitic and basaltic lavas

Component[a,b]	Perserverance komatiite	Kambalda komatiite	Cape Smith kom. basalt	Lunar mare basalt	Tholeiitic basalt
SiO_2	45.0	45.5	46.9	43.8	50.9
TiO_2	0.4	0.3	0.6	2.6	1.7
Al_2O_3	7.2	6.6	9.8	7.9	14.6
Fe_2O_3	1.5	1.6	–	–	–
FeO	10.1	9.9	14.4	21.7	14.6
MnO	0.2	0.2	0.3	0.3	–
MgO	29.4	29.0	18.9	14.9	4.8
CaO	6.2	6.2	8.6	8.3	8.7
Na_2O	0.02	0.6	0.3	0.2	3.1
K_2O	0.03	0.04	0.05	0.05	0.8
T_{liq} (°C)	1590	1590	1420	1440	1160
T_{sol} (°C)	1170	1170	1150	1150	1080
ρ at T_{liq} (kg/m^3)	2780	2770	2800	2900	2750
c (J/kg °C)	1760	1760	1640	1570	1480
μ at T_{liq} (Pa s)	0.11	0.12	0.74	0.40	86
L at T_{liq} (J/kg)	6.76×10^5	6.75×10^5	5.96×10^5	6.06×10^5	5.37×10^5
k at T_{liq} (J/m s °C)	0.4	0.4	0.5	0.5	0.7
h (m)	10	10	10	10	10
u at T_{liq} (m/s)	5.0	4.9	3.9	4.2*	1.7
Re at T_{liq}	2.43×10^6	2.33×10^6	1.46×10^5	3.09×10^5*	5.50×10^2
Pr at T_{liq}	5.23×10^2	5.37×10^2	2.6×10^3	1.3×10^3*	1.9×10^5
h_r at T_{liq} (J/m^2 s °C)	630	620	172	217*	n/a
u_{mb} at T_{liq} (m/day)	2.4	2.5	0.52	0.24*	n/a
Composition location	Perseverance, Western Australia	Kambalda, Western Australia	Katinniq, Cape Smith Belt, Canada	Apollo 12 Sample 12002	Columbia River Basalt, Washington
Composition reference[c]	1	2	3	4	5

[a] T_{liq} = liquidus temperature, T_{sol} = solidus temperature, ρ = density, c = specific heat, μ = dynamic viscosity, L = heat of fusion, k = thermal conductivity, h = flow thickness, u = flow velocity, Re = Reynolds number, Pr = Prandtl number, h_r = convective heat transfer coefficient, u_{mb} = thermal erosion rate of consolidated basalt, * = if erupted on Earth, n/a = not applicable for non-turbulent flows.

[b] For all compositions, liquidus temperature was calculated using MELTS (Ghiorso and Sack, 1995). The solidus temperature for komatiite is from Arndt (1976) and is estimated for all other compositions. Liquid density was calculated using the method of Bottinga and Weill (1970) with the partial molar volume data of Mo et al. (1982), liquid viscosity was calculated using the method of Shaw (1972), specific heat was calculated from the heat capacity data of Lange and Navrotsky (1992), and heat of fusion for komatiite liquids is approximated using curve fits to the data of Navrotsky (1995). Thermal conductivity was calculated using the exponential equation from Fig. A1, which is a curve fit to the conductivity data of Murase and McBirney (1973).

[c] References: (1) Normalized average of Perseverance spinifex komatiites WAP111-495.1, WAP111-491, and WAP111-490.5; (2) Kambalda komatiite (adapted from Lesher and Arndt, 1995); (3) Katinniq komatiitic basalt (Barnes et al., 1982); (4) Apollo 12 sample 12002 (Walker et al., 1976); (5) Columbia River basalt (Murase and McBirney, 1973).

moon Io (e.g. McEwen et al., 1998), and work is underway to investigate the relationships between these materials and terrestrial komatiites (Williams et al., 2000).

2.2. Previous work on the Perseverance Ultramafic Complex

Perseverance is located 380 km NNW of Kalgoorlie in the Norseman–Wiluna greenstone belt of Western Australia (Fig. 1). It represents one of the largest economic accumulations of komatiite-associated massive and disseminated magmatic Ni–Cu sulfide mineralization in the world (Libby et al., 1998). The Perseverance Ultramafic Complex (PUC) itself (Fig. 2) is a regionally extensive, lens-shaped unit of coarse-grained olivine mesocumulate to adcumulate komatiite overlying a thick substrate of dacitic tuff. U–Pb dating of zircons in the felsic rocks adjacent to the Perseverance Ultramafic Complex yield an age of 2720 ± 14 Ma (D. Nelson, pers. commun. to J. Libby, 1996).

Barnes et al. (1988a,b) studied the stratigraphy and structural geology of the area, and concluded that the Perseverance Ultramafic Complex consisted of a 2–3-km-wide lenticular body of olivine adcumulate komatiite, originally at least 500 m thick, flanked by laterally extensive, thinner sequences of olivine orthocumulate and spinifex textured rocks. Based on stratigraphic relationships in the underlying rocks they concluded that the base of the adcumulate lens transgressed at least 100 m of footwall stratigraphy, and that the adcumulates occupied a channel formed by extensive thermal erosion by a turbulently-flowing, high MgO komatiite lava river. Subsequent work by geologists from WMC Ltd (Libby et al., 1998), based on more extensive underground mapping and drilling, highlighted the importance of structural modification of the mine geology. A modified interpretation of the geological relationships at the base of the lens, taking account of the Libby et al. (1998) observations, is presented by Barnes et al. (1999). The mineralized flow units, originally interpreted by Barnes et al. (1988b) to have been separated from the base of the adcumulate lens by 100–150 m of volcanogenic sediments, are now believed to have originally been directly overlain by adcumulate and to have been subsequently separated from it by a major dextral shear zone. Under this interpretation, it is not possible to make a reliable estimate of the magnitude and morphology of the original embayment, but the interpretation that at least 100 m of footwall stratigraphy is truncated by the base of the adcumulate is still valid (Fig. 3).

Most of the original igneous structures and textures in the Complex have been variably modified by post-emplacement tectonic deformation and metamorphism, including serpentinization (Donaldson, 1982), carbonate alteration (Gole et al., 1987), and crystallization of metamorphic olivine (Barnes et al., 1988a). Thus, although igneous cumulate textures are usually well preserved, especially away from contacts and faults (Libby et al., 1998), the thicknesses of individual komatiite flows (i.e. individual cooling units) are difficult to determine in most areas. There has been some structural displacement along the base and top of the embayment containing the PUC (Fig. 3), especially along the Perseverance and 60A faults. The adjacent Rocky's Reward ultramafic unit, which was originally interpreted as an independent body (Barnes et al., 1988b), is now considered to be an attenuated tectonic slice off the bottom of the PUC (Libby et al., 1998). Komatiite flows in the better preserved Rocky's Reward unit have been estimated to be ~30–40 m thick, although the initial flow thickness may have been as little as 10 m. These thin flows are thought to have undergone inflation (see Hon et al., 1994) to form the thick adcumulate pile (Barnes et al., 1999).

Libby et al. (1998) concluded that only minor modifications were required to the emplacement model of Barnes et al. (1988a). In particular, instead of two separate komatiite eruptive episodes that formed the massive and disseminated sulfide units (Barnes et al., 1988a), Libby et al. (1998) suggested that the PUC represents a large channel(s) that formed during a single, major eruptive event that underwent episodic variation in emplacement conditions (e.g. flow rate, degree of turbulence, temperature, thermal erosion). Initial development involved thermal erosion, precipitation of sulfides, and crystallization of olivine in a wide channelized sheet flow. A variation in eruption conditions (higher thermal erosion, more contamination and massive sulfide production) permitted the development of a subchannel that contained the large volume of immiscible massive

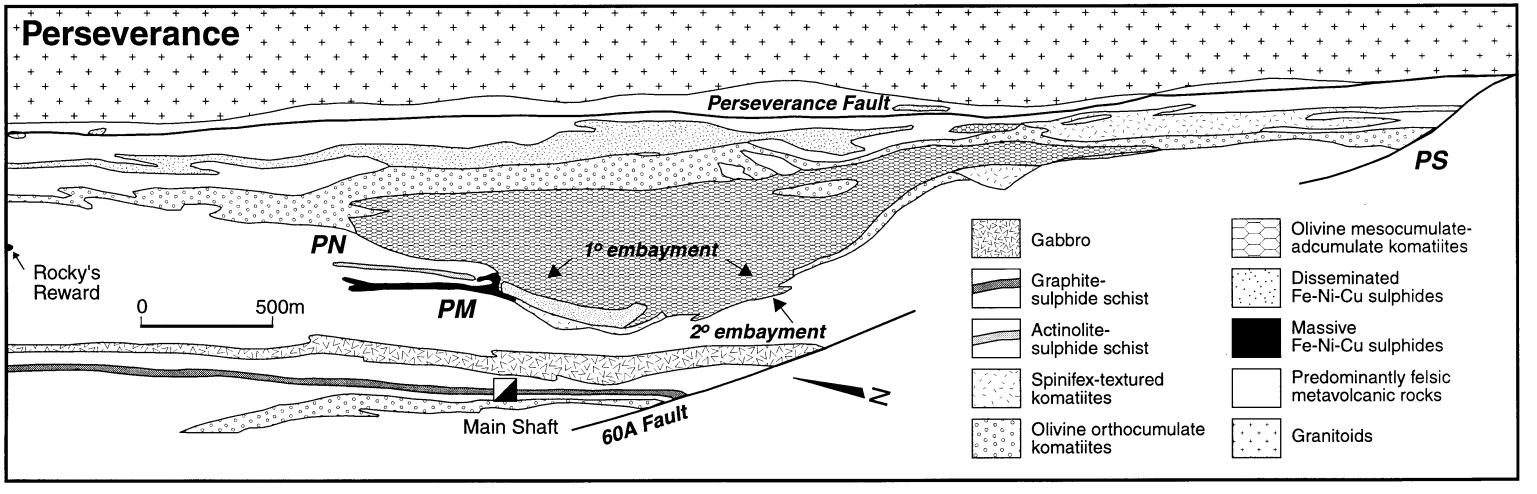

Fig. 2. Geologic map of the Perseverance Ultramafic Complex, Western Australia. After Barnes et al. (1988a).

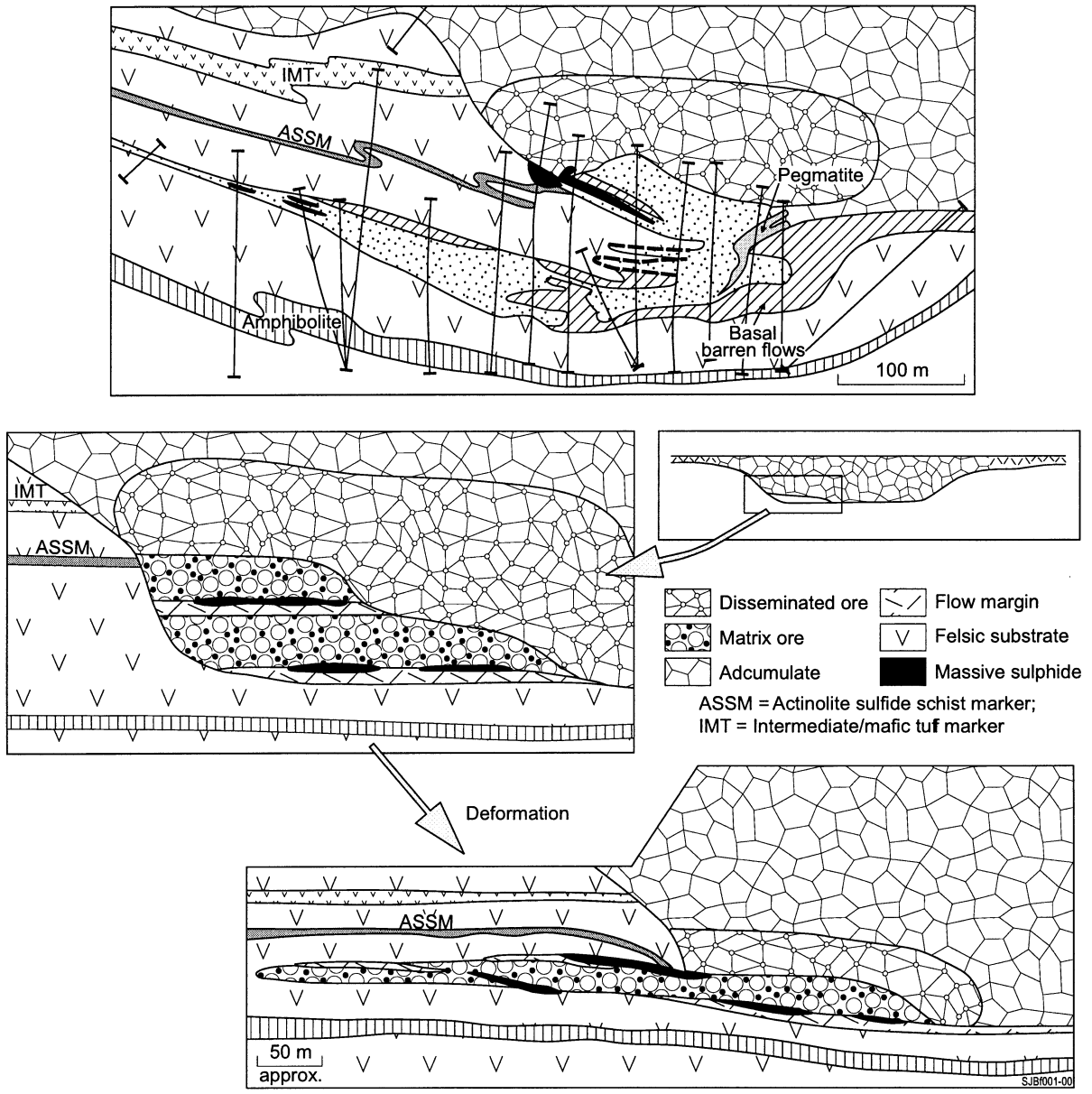

Fig. 3. Interpretive reconstruction of the Perseverance embayment based on the recent work of Libby et al. (1998).

sulfide that accumulated at its base, whereas the more extensive (less turbulent?) zone above contained lavas that accumulated in weakly to moderately disseminated sulfides (Libby et al., 1998). This interpretation is consistent with theories of the formation of channelized sheet flows (Lesher and Arndt, 1995) and the development of preferred pathways (i.e. lava tubes) in sheet flows (e.g. Peterson et al., 1994; Hill et al., 1995).

The majority of komatiite-hosted nickel deposits in the Norseman–Wiluna Belt outside the Kambalda and Widgiemooltha area have felsic substrates. This includes Perseverance, Silver Swan, Cosmos, Mt Keith, and Cliffs. Felsic volcanic and epiclastic

rocks extend throughout the Agnew–Wiluna segment of the belt over a strike length of 150 km from Perseverance to Wiluna. The substrate to the PUC comprises feldspar–phyric, dacitic to rhyolitic crystal tuffs with calc-alkaline geochemical affinities, intercalated with more mafic, possibly tuffaceous units and a prominent marker horizon, the actinolite–sulfide schist, a 1–2 m thick layer containing at least 50% pyrrhotite (Barnes et al., 1988a, 1995). This unit is strongly mylonitized, but appears to represent an original stratigraphic unit. The felsic tuffs are strongly metamorphosed and locally deformed, and no sedimentological studies (e.g. grain size determinations, porosity estimates, etc.) have been undertaken. Although the original nature of the groundmass component is obscured by metamorphic recrystallization, the phenocryst component of the tuffs appears to have been coarse sand sized. Because it is reasonable to assume that both the phenocryst and groundmass components of the tuff have increased in grain size during prograde metamorphism, this is probably a maximum grain size. The source of these tuffs is also unknown; they could have come from subaqueous pyroclastic flow deposits that may or may not have been welded (see Sparks et al., 1980), or they could have come from subaqueous unconsolidated pyroclastic fall deposits. It is also unclear what was the S source for the Fe–Ni–Cu sulfides at Perseverance. In the current interpretation, the actinolite sulfide marker is an example of the type of sulfidic footwall materials that could have contributed S to the formation of the deposit.

Relict igneous olivine is common in the core of the adcumulate lens, and exhibits a progressive increase in forsterite content over a distance of 500 m, from $Fo_{92.8}$ in the basal cloud sulfide zone to $Fo_{94.4}$ in the uppermost preserved stratigraphic level. Based on these data and the analysis of flanking spinifex-textured rocks with well preserved igneous textures, Barnes et al. (1988a) inferred that the most magnesian Perseverance komatiite liquids contained up to 33% MgO. Nisbet et al. (1993) argued that the maximum MgO contents of Archean komatiites were ≤28%, on the grounds that higher values would require much higher mantle potential temperatures, and that the spinifex samples at Perseverance must be metasomatized or enriched in accumulated olivine. Further analysis of the Perseverance data reveals that compositions of flanking olivine spinifex-textured rocks, which could be in equilibrium with Fo_{94}–$Fo_{94.5}$ olivines, fall in the range 27–31% MgO (assuming 10% of total Fe as Fe_2O_3), so 29% MgO is adopted here as a conservative estimate of the MgO content of the most primitive lava erupted at Perseverance.

In regards to contamination of the Perseverance komatiites from surficial thermal erosion and assimilation of melted felsic tuff, Barnes et al. (1988a) reported apparently high levels of lava contamination (later estimated to be ~10–20% by Barnes et al., 1995, on the basis of LREE enrichment) in the ~30-m-thick flows at Rocky's Reward and in the Perseverance Mineralized Flows, as well as in the thinner flanking flows in the Perseverance Ultramafic North area. Barnes et al. (1995) suggested that continuous surficial thermal erosion of the thick felsic substrate by komatiite lava would produce these highly contaminated lavas as long as the komatiite lava remained hot enough and flowed fast enough to remove substrate. This degree of contamination is much greater than the 2–5% estimated for the Kambalda komatiites (Lesher and Arndt, 1995), presumably because the quantity of felsic sediment near the lava source available to contaminate the Kambalda komatiites was much less than at Perseverance (see discussion by Lesher and Stone, 1996; Williams et al., 1998; Lesher et al., 2001a). We have considered the possibility that the LREE enrichment at Perseverance might be due to mobility of LREE from the surrounding felsic rocks during post-emplacement metamorphic processes. Because of their low initial REE contents, dunites would be particularly susceptible to alteration. However, recent geochemical work (C.M. Lesher and S.J. Barnes, unpublished data) indicates that many, but not all, Perseverance samples are enriched not only in LREE, but also in U and Th, and exhibit mantle-normalized incompatible element patterns with pronounced negative Nb anomalies, a geochemical signature that is characteristic of crustal contamination. It is possible that there has been some mobility of LREE during metamorphism, but U, Th, and Nb are normally much less mobile in metamorphic fluids because of their greater valences and smaller ionic radii. The inferred level of contamination at Perseverance (~10–20%: Barnes et al., 1995) is the

highest ever reported in komatiite lava flows,[1] and as we shall see, it is one of the factors that can be used to constrain our modeling of komatiite lava emplacement and thermal erosion at Perseverance.

Given this information on the field geology of the Complex and hypotheses on its mode of formation, it is possible to physically model emplacement of komatiite lavas and thermal erosion at Perseverance.

3. Analytical/numerical modeling

3.1. Previous modeling

The technical description of our model of komatiite emplacement and its application to the Kambalda flows were published in Williams et al. (1998, 1999a) and are included in Appendices A and B; preliminary modeling results for Perseverance were published in Williams et al. (1999a). Our model, which has since been slightly modified as described in Appendix B, simulates the thermal, rheological, fluid dynamic, and geochemical evolution of a komatiite flow during emplacement. Beginning with a set of initial conditions (lava eruption, liquidus, and solidus temperatures, lava and substrate major oxide compositions, flow thickness, ground slope, ground melting temperature, and ambient temperature), the thermal and physical properties of the lava are calculated at the vent using a series of algorithms from experimental petrology (see Table 1 and Appendix A). These parameters are used to numerically solve a first-order ordinary differential equation for lava temperature as a function of distance downstream. In this equation, the lava temperature decreases both by convective heat loss in the lava to the top and bottom of the flow and by the assimilation of cold material thermally eroded from the base of the flow, but this decrease is reduced by the latent heat released during olivine crystallization. At each distance increment, a series of equations are used to recalculate the viscosity, crystallinity, flow velocity, Reynolds number, Prandtl number, convective heat transfer coefficient, thermal erosion rate, degree of lava contamination, and crustal thickness (assuming crustal growth is constrained by convection to cold sea water from the upper flow surface), as well as the compositional changes in lava composition due to assimilation of substrate and crystallization of olivine. Thus, the physical and geochemical changes in the flow can be assessed.

Our basic model (Appendix A) assumes an anhydrous, consolidated substrate. Because the Kambalda embayments are thought to have once contained a fine-grained, water-saturated, unconsolidated sediment, Williams et al. (1998) developed a thermomechanical erosion model that assumed heat from the lava would vaporize intergranular sea water in the sediment (see also Appendix A). This water vapor would have the capability to fluidize sufficiently small particles ($\leq$0.1 mm, very fine sand or smaller), causing disaggregation of the sediment (Kokelaar, 1982). Williams et al. (1998) demonstrated that this process of combined thermal–mechanical erosion could have produced much higher erosion rates ($\sim$20 m/day) and degrees of contamination ($\geq$10%) than thermal erosion of consolidated rocks. As we shall see, because of the poorly-defined nature of the Perseverance tuffaceous substrate, models for erosion of consolidated, partly consolidated, and unconsolidated materials are necessary to understand the style of lava emplacement at Perseverance.

3.2. Model assumptions and refinements for Perseverance

Many assumptions about the compositional and physical nature of Archean komatiites and the environments into which they flowed are required to model their emplacement. As such, our model results are useful only as long as these assumptions are valid. Because of the large number of unknowns involved in modeling Archean komatiite flows, the precise figures of our model results are probably less important than the order of magnitude of the results. Thus, we caution readers to evaluate our results with a practical rather than dogmatic view.

In general, we assume komatiites erupted hot (at their liquidi), flowed turbulently, and had thermally-mixed and homogenous interiors. We assume submarine emplacement at a depth of ~1 km below sea level

[1] High-Mg basalts overlying the Kambalda Komatiite Formation are interpreted to have formed up to 25% contamination of Kambalda komatiite by granitic material, but this is thought to have occurred by thermal erosion during ascent through the continental crust (Arndt and Jenner, 1986).

(pressure ~100 bars), on an ocean floor that is gently sloping (with a slope ~0.1°). We assume this floor had no topographic variations, and was homogenous in composition. We assume that an insulating crust forms quickly and is relatively stable during turbulent emplacement (e.g. like the fragmental crusts on modern 'a'a flows (Keszthelyi and Self, 1998), or alternatively, like the winter ice cover on turbulently flowing rivers). We assume convective heat transfer in the turbulent lava (Huppert et al., 1984; Huppert and Sparks, 1985a,b), which is modeled using a heat transfer coefficient for turbulent pipe flows (see Appendix A). There are a variety of uncertainties involved with these coefficients (see Section 6.4 of Williams et al., 1998), including the effect of surface roughness on heat transfer, which are not addressed in this work.

To model lava emplacement at Perseverance, because of the ambiguous nature of the Perseverance Ultramafic Complex, more specific assumptions are required. First, there are few constraints on the original flow thickness of the Perseverance lavas. The Rocky's Reward ultramafic unit, which may have once been part of the PUC, appears to have basal flows with thicknesses of ~30–40 m. On the other hand, the modeling of Jarvis (1995) suggests that lava channels similar to Perseverance, which have a concave cross-sectional morphology, should have formed by thermal erosion of flows whose thickness is greater than or equal to the depth of erosion (i.e. no undercutting), which would constrain Perseverance flow(s) to a thickness $\geq$100 m. However, a water-saturated sediment under 100 bars pressure should have a lower cohesive strength than typical consolidated ocean floor rocks such as basalts, which when undercut probably would result in collapse of the overlying material, causing the channel to return to a concave cross-sectional morphology. There is evidence that this may have occurred at Katinniq in northern Québec, where sediment-basalt breccias with hornfelsed fragments and unhornfelsed matrix flank the lava channel (Gillies and Lesher, 1992; Lesher et al., 1999, 2001a,b). If this occurred at Perseverance, the absence of breccias would imply that any collapsed material was assimilated. Additionally, although we assume constant flow rates in our modeling (so that thickness increases as velocity decreases), we cannot dismiss the possibility of Hawaiian-style flow inflation (e.g. Hon et al., 1994), such that the flow thicknesses measured in the field might not represent the original flow thicknesses. Inflation in komatiite flows has recently been reported (Dann, 2000). Because of these uncertainties, we have modeled Perseverance using a range of initial flow thicknesses: 10, 30, and 100 m.

Second, as discussed in Section 2.2, the MgO content of the Perseverance lavas is debatable. Because higher degrees of contamination (such as those estimated for the Perseverance lavas) can be expected to occur with higher MgO komatiites, and the range of MgO contents of the original Perseverance lavas is thought to fall between 27 and 31%, we have utilized a conservative value of ~29% MgO lava composition for our modeling of Perseverance (Table 1). We have also performed several model runs using a ~31% MgO composition, to gauge the effect of more ultrabasic lavas on flow emplacement. We also assume the high levels of lava contamination estimated for Perseverance (~10–20%) are due to surficial thermal erosion, and not due to assimilation of crustal material during ascent. This assumption is supported by the localized nature of the contamination (Barnes et al., 1995).

Third, because the original degree of consolidation of the tuffaceous substrate is unclear, we need to model thermal erosion at Perseverance using several endmember cases. Our existing models can simulate thermal erosion of either an anhydrous, consolidated tuff, or a hydrous, unconsolidated tuff. A third possibility is a hydrous, partly consolidated or welded tuff, as welded tuffs can occur in subaqueous pyroclastic deposits (Kokelaar and Busby, 1992; Fritz and Stillman, 1996). Theoretically, a welded felsic tuff (which can have significant porosity) should only require some fraction of the heat of fusion to melt the matrix of the tuff before the remainder can be removed by mechanical erosion. In this case, the energy to melt the ground is given by:

$$E_{mg} = (1 - f_w)\{\rho_g[c_g(T_{mg} - T_a) + f_L L_g]\} + f_w\{\rho_w[c_w(T_{vap} - T_a) + L_{vap}]\} \quad (1)$$

in which f_L is the fraction of the heat of fusion required to melt the matrix of the tuff (a complete list of symbols is given at the end of the paper). The erosion

rate is given by:

$$u_m = \frac{h_T(T - T_{mg})}{E_{mg}} \quad (2)$$

The primary energy conservation equation for lava emplacement under these conditions, assuming that the steam that is lost from the pore spaces in the welded tuff is further heated by the lava (up to lava temperature T) takes the form:

$$\rho_b c_b h u \frac{dT}{dx} = -h_T(T - T_{mg}) - h_T(T - T_{sol}) - \frac{h_T(T - T_{mg})E_{hg}}{E_{mg}} + \rho_b c_b h u \frac{dT}{dx}\left(\frac{L_l x'(T)}{c_b}\right) \quad (3)$$

in which the energy to heat the ground is given by:

$$E_{hg} = [(1 - f_m)\rho_g\{c_g(T - T_{mg}) + (1 - f_L)L_g\} + f_w\rho_{vap}c_{vap}(T - T_{vap})] \quad (4)$$

in which ρ_{vap}~55 kg/m^3 and c_{vap}~6900 J/kg °C. We will assume the tuff has a porosity of 50%, which is filled with sea water. This is consistent with the porosities of modern submarine felsic tuffs and hyaloclastities (~50% at sea floor: Schmincke et al., 1995).

Additional assumptions are required for a welded tuff model. First, there is no information on the fractional heat of fusion (f_L) required to unweld tuff particles. Second, the viscosity of a steam/melt substrate mixture is unknown, and there is a variation of at least nine orders of magnitude between the endmembers (i.e. μ_{vap}~0.000021 Pa s, μ_{melt}~13,400 Pa s). Third, there is uncertainty about the effective melting temperature of a tuff that consists of unknown fractional amounts of both crystals (~910°C) and felsic glass particles (~600–750°C: see Ryan and Sammis, 1981; Westrich et al., 1988). We have chosen to model a welded tuff assuming a best case to maximize thermal erosion, assuming f_L~0.2, μ_g~10 Pa s, and T_{mg}~700°C. The choice of 20% for the fraction of latent heat required to disaggregate a partly consolidated tuff is simply an estimate for a parameter that has never been determined experimentally. The choice of ~10 Pa s, as the substrate melt viscosity is intermediate in the range of endmembers given above. The choice of 700°C is within the effective melting temperature range for a glass and crystal tuff.

Lastly, a sensitivity analysis of our model was performed, and is summarized in Williams et al. (1999a). Briefly, the properties of lava flow rate (initial flow thickness), lava composition, substrate composition and degree of consolidation (including intergranular water), eruption temperature, and ground slope are most important for affecting model output, and good starting values of these parameters are required for robust modeling. In general, with all else equal, thermo-mechanical erosion increases for thicker komatiite flows, for more magnesian flows, for more felsic, less consolidated, more water-rich substrates, for higher eruption temperature (including superheated) flows, and for flows down steeper slopes.

With consideration of all the uncertainties and complications discussed above, we have attempted to model komatiite lava emplacement at Perseverance, with a goal of determining the eruption requirements for producing thick, highly contaminated komatiite flows. Because we have independent geochemical modeling data suggesting the Perseverance lavas were contaminated ~10–20% (Barnes et al., 1995), we calculated the flow distance, thermal erosion rate, etc. for our model predictions within that range of contamination.

4. Results

We present our modeling results (Figs. 4–6; Table 2) as several case studies, each assuming either a liquidus or superheated lava flow over a felsic tuff substrate with a different degree of consolidation.

4.1. Case 1: liquidus lava over consolidated substrate

Case 1 involves komatiite flows erupted at their liquidus temperatures over a dry, consolidated felsic tuff (Fig. 4). For all flow thicknesses (i.e. flow rates), it is not possible to obtain levels of contamination >10% prior to the cessation of turbulent flow (Re = 2000). In general, our modeling shows that

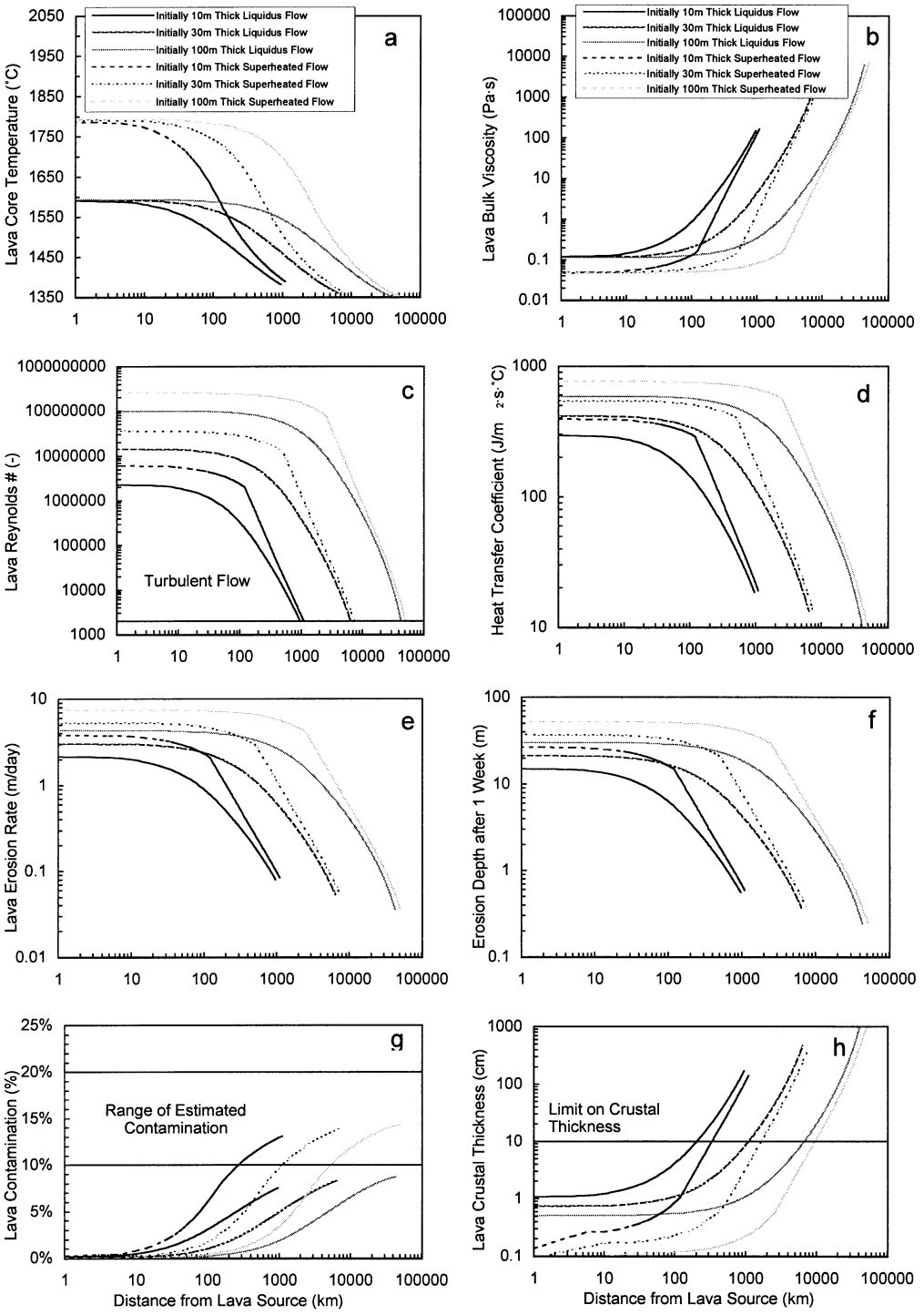

Fig. 4. Model results for the emplacement of 29% MgO, liquidus and superheated Perseverance komatiite flows over dry, consolidated tuff.

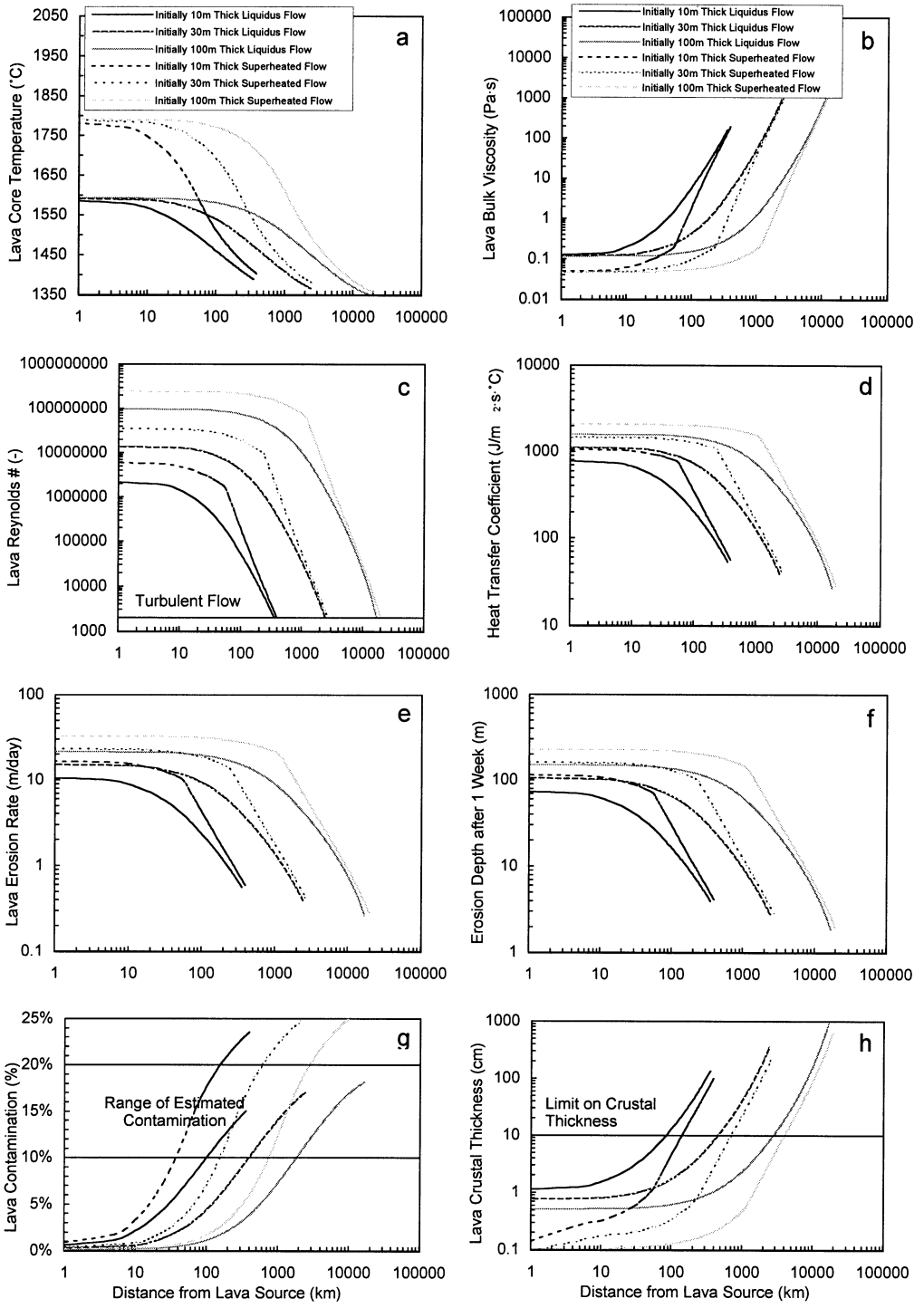

Fig. 5. Model results for the emplacement of 29% MgO, liquidus and superheated Perseverance komatiite flows over wet, partly consolidated (welded) tuff.

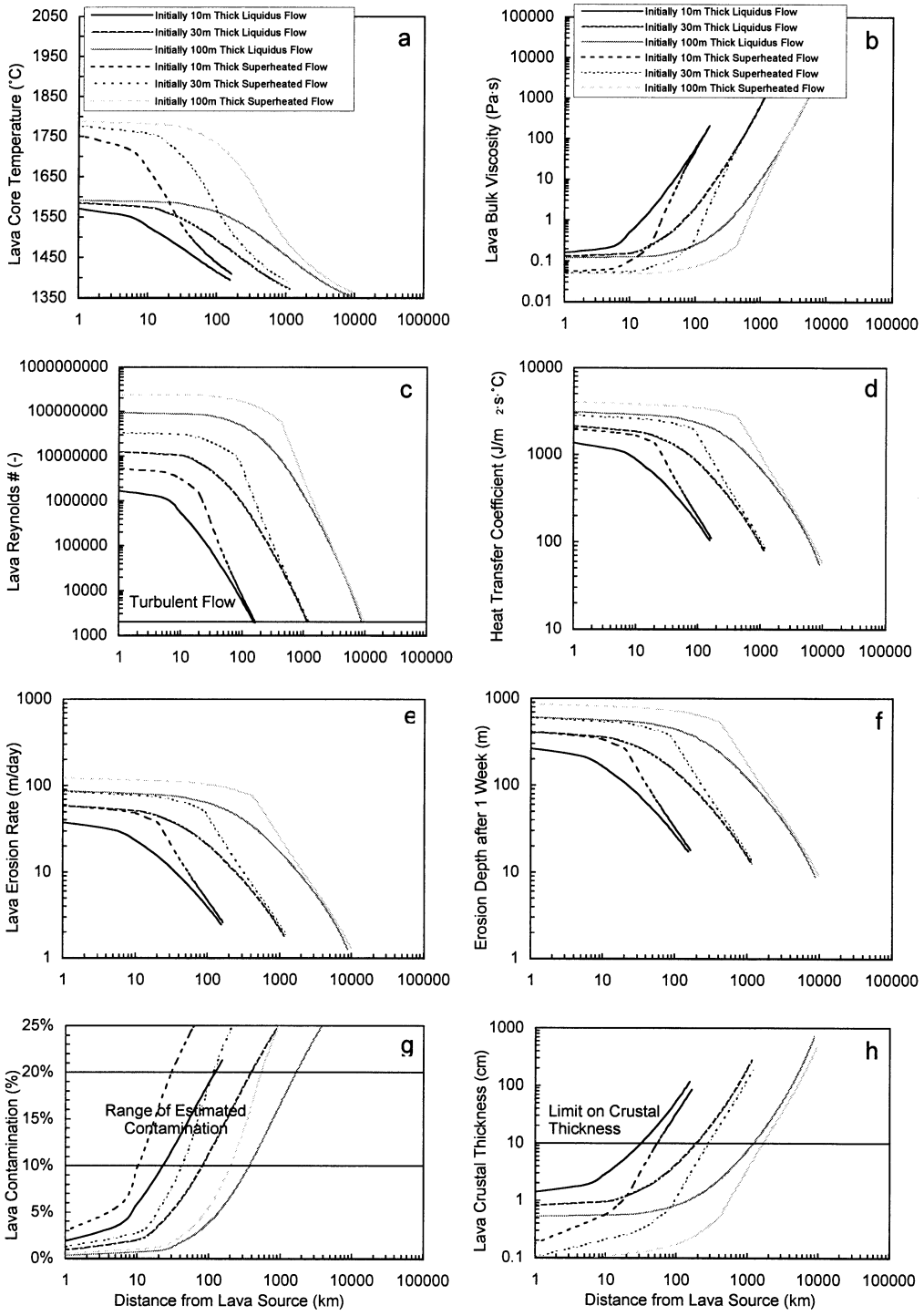

Fig. 6. Model results for the emplacement of 29% MgO, liquidus and superheated Perseverance komatiite flows over wet, unconsolidated tuff.

Table 2
Model results for the emplacement of 29% MgO Archean komatiite lava flows at Perseverance, W.A

Property (units)	Initially 10 m thick flow	Initially 30 m thick flow	Initially 100 m thick flow
Liquidus lavas over dry, consolidated tuff			
Max. flow distance[a] (km)	965	6460	43,100
Max. flow thickness[a] (m)	19	61	220
Max. erosion rate[b] (m/day)	2.2	3.1	4.3
Max. erosion depth after 1 week[a] (m)	16	22	30
Max. contamination[a] (%)	7.5	8.3	8.7
Max. crustal thickness[a] (cm)	170	460	> 1100
Superheated lavas over dry, consolidated tuff			
Max. flow distance[a] (km)	1100	7410	50,900
Max. flow thickness[a] (m)	20	67	240
Max. erosion rate[b] (m/day)	3.9	5.4	7.5
Max. erosion depth after 1 week[b] (m)	27	38	53
Max. contamination[a] (%)	13	14	14
Max. crustal thickness[a] (cm)	140	370	920
Liquidus lavas over wet, welded tuff			
Max. flow distance[a] (km)	355	2450	17,060
Max. flow thickness[a] (m)	20	66	240
Max. erosion rate[b] (m/day)	11	15	22
Max. erosion depth after 1 week[b] (m)	78	110	150
Max. contamination[a] (%)	15	17	18
Max. crustal thickness[a] (cm)	140	350	920
Superheated lavas over wet, welded tuff			
Max. flow distance[a] (km)	40–150	160–600	760–2780
Max. flow thickness[a] (m)	11–16	34–45	112–140
Max..erosion rate[b] (m/day)	17	24	33
Max. erosion depth after 1 week[b] (m)	120	160	230
Max. contamination[a] (%)	10–20	10–20	10–20
Max. crustal thickness[a] (cm)	0.8–11	0.5–6.9	0.3–4.2
Liquidus lavas over unconsolidated tuff			
Max. flow distance[a] (km)	25–125	90–390	380–1660
Max. flow thickness[a] (m)	13–19	37–50	120–160
Max. erosion rate[b] (m/day)	49	67	95
Max. erosion depth after 1 week[b] (m)	340	470	660
Max. contamination[a] (%)	10–20	10–20	10–20
Max. crustal thickness[a] (cm)	7.4–79	3.8–30	2.2–16
Superheated lavas over unconsolidated tuff			
Max. flow distance[a] (km)	15–30	50–120	220–540
Max. flow thickness[a] (m)	12–14	34–40	110–130
Max. erosion rate[b] (m/day)	69	95	130
Max. erosion depth after 1 week[b] (m)	480	660	930
Max. contamination[a] (%)	10–20	10–20	10–20
Max. crustal thickness[a] (cm)	0.8–3.0	0.5–1.7	0.3–0.9

[a] As turbulent flow, limit at Reynolds number = 2000.
[b] At vent.

thicker flows travel longer distances (thermally eroding as they go) to build up higher levels of contamination than thinner flows. For example, suppose we assume that the maximum geologically-reasonable distance[2] for a submarine turbulent flow is 1000 km. Then, for an initially 100-m-thick flow, the degree of contamination at this distance is 1.9%. The erosion rate at this distance is 2.7 m/day, which would require an eruption duration of 37 days (>1 month) to erode a 100-m-deep Perseverance-like embayment in consolidated tuff, with a resulting flow volume of 1.6×10^4 km^3. This result falls between the maximum average volume/flow found in the Columbia River Flood Basalt Province (~2.1×10^3 km^3) for the N1 Grande Ronde Flow: Tolan et al., 1989) and the total volumes of oceanic plateaus such as Ontong Java (>5×10^7 km^3: Mahoney, 1987; Coffin and Eldholm, 1993). These figures need not be considered significant, however, because the low amount of contamination produced in this model suggests that Perseverance could not have resulted from the emplacement of liquidus lava over a consolidated tuff.

4.2. Case 2: superheated lava over consolidated substrate

One method of increasing erosion rate and lava contamination at flow distances closer to the vent is by erupting superheated lavas. Although the dunitic rocks in the PUC clearly crystallized at or near their liquidus temperature, these rocks do not record the temperature at the eruption site (which would have been higher upstream), nor the temperature of the lava that initially flowed through the channel (which would have been flushed downstream as the channel continued to flow and crystallize). Lesher and Groves (1986) argued that low-viscosity komatiites should have ascended very rapidly along P–T trajectories steeper than the adiabat, and that many, if not most, should have been superheated on eruption. If so, this would increase the amount of thermal erosion near the eruptive site, but the lavas would quickly cool with increasing distance, limiting the ability of this to explain, by itself, the high degrees of contamination at Perseverance.

For example, when an initially 100-m-thick komatiite lava is superheated to 200°C above its liquidus temperature, the degree of lava contamination at a distance of 1000 km downstream increases to 3.4% (Fig. 4). However, this is still far short of that determined for the Perseverance lavas. Contamination of 10% is attained at a distance >5200 km from the lava source, which is probably not geologically reasonable. Even at this distance, the model lava erosion rate is 1.4 m/day, which is insufficient to produce a ~100-km-deep erosion channel for an eruption duration of less than a few months. Thus, if the tuff underlying Perseverance was consolidated and anhydrous, it seems unlikely that even a superheated komatiite could have formed the embayment by thermal erosion.

4.3. Case 3: liquidus lava over partly-consolidated (welded) substrate

Case 3 involves liquidus komatiite flow over a hydrous (50% H_2O), partly-consolidated (welded) felsic tuff. Here, we assume that only 20% of the heat of fusion of the substrate is required to unweld the tuff,[3] which along with the substantial water fraction in the substrate should result in higher erosion rates and degrees of contamination at a given distance from the source. This hypothesis is verified by the following model results. For an initially 100-m-thick flow, our modeling (Fig. 5) suggests that contamination of ~10% is attained at a distance of ~1800 km from the source, where the erosion rate is ~5.5 m/day. This erosion rate would have required an eruption duration of ~18 days (>2 weeks) to remove 100 m of welded tuff, with a resulting flow volume of ~7940 km^3, over three times the maximum average volume per flow of the largest CRB flow units (2093 km^3: Tolan et al., 1989) but less than the estimated volumes of flood basalts in oceanic plateaus (>10^6–10^7 km^3: see Mahoney and Coffin, 1997, and references therein). Although our modeled flow

[2] Although lava channels ≥1000 km are not found on Earth, some extraterrestrial lava channels are thousands of kilometers long. For example, Hildr Fossa on Venus is a long, canali-type lava channel that is continuous for over 6800 km in length (Head et al., 1991). The composition and emplacement conditions that produced this channel are unknown.

[3] This parameter is unknown, but has been estimated assuming that the tuff crystals were anhedral, moderately well sorted, and loosely packed.

volumes may not be unrealistic, the flow distances seem unlikely.

Up to this point, we have not discussed the potential role of thinner (<100 m) flows in the production of Perseverance. As we indicated, the numerical modeling of Jarvis (1995) suggests erosion channels with a concave cross-sectional morphology similar to Perseverance form from flows thicker than the channel depth. In contrast, for flows whose upper surface sinks below the base level of the ground, thermal erosion from the sides (i.e. undercutting) results in a reentrant morphology (see also Huppert and Sparks, 1985a). These studies assumed a massive, homogeneous, consolidated substrate. In the case of Perseverance, an undercut lava channel in water-saturated, poorly-consolidated sediment might collapse, resulting in a concave cross-sectional morphology. Libby et al. (1998) suggested that the structural deformation at Perseverance was so intense that the original morphology of the embayment could have been altered, perhaps from a reentrant form.

If we accept that the concave embayment formed from one or more thinner flows by undercutting and the collapse of a nascent reentrant embayment, our modeling suggests that they could have been contaminated up to 10–20% much closer to the source. For example, an initially 30-m-thick flow would reach a contamination level of ~10% at a distance of ~400 km from the source, where an erosion rate of ~3.6 m/day would have required an eruption duration of ~28 days (<1 month) to remove 100 m of welded tuff. In this case, the resulting flow volume is ~1790 km^3, within the range of the average volume/flow of the Columbia River flood basalt flows (5–2093 km^3: Tolan et al., 1989). For an initially 10-m-thick flow, a contamination level of ~10% is attained at a distance of ~100 km downstream, where an erosion rate of 2.3 m/day would have required an eruption duration of ~43 days to remove 100 m of welded tuff, with a corresponding flow volume of ~370 km^3. Thus, if thinner flow(s) formed a reentrant Perseverance embayment that collapsed to a concave form, then liquidus lavas with thicknesses consistent with observed Perseverance flows could have produced a larger thermal erosion channel and highly contaminated lavas <500 km from the source with eruption volumes not unlike modern flood basalt eruptions.

4.4. Case 4: superheated lava over partly-consolidated (welded) substrate

For an initially 100-m-thick, superheated komatiite lava over a partly-consolidated substrate (Fig. 5), our modeling suggests that contamination of 10% can be attained at a flow distance of ~760 km from the source, where a high erosion rate (~23 m/day) occurs. Although these turbulent flow distances might still be unreasonably long, our results show that a wet welded tuff is more erodable than a dry, consolidated tuff, and that lava superheating can substantially increase thermal erosion and contamination. At a distance of 760 km and with an erosion of 23 m/day, our initially 100 m thick komatiite flow could produce a 100 m deep embayment in the welded tuff in ~4.4 days. With a flow rate of 5.4×10^6 m^3/s, this eruption might have a volume of ~2040 km^3, similar to the N1 Grande Ronde flow in the CRB (~2093 km^3: Tolan et al., 1989).

As observed in the results for thinner liquidus flows, thinner superheated flows can become highly contaminated much closer to the source. For example, an initially 30-m-thick, superheated komatiite flow would attain a contamination of 10–20% at a distance of 160–600 km downstream from the eruption source. Erosion rates at these distances range from 16 to 3.7 m/day which would require eruption durations of ~6.3–27 days to remove 100 m of welded tuff. With a flow rate of ~7.8×10^5 m^3/s and this eruption duration, a flow volume of ~430–1830 km^3 is predicted. This range of flow volumes is consistent with the average volume/flow of CRB flow units (5–2093 km^3: Tolan et al., 1989). For an initially 10-m-thick flow, a contamination level of ~10–20% is attained at a distance of ~40–150 km downstream, where an erosion rate of 12–2.4 m/day would have required an eruption duration of ~8–42 days to remove 100 m of welded tuff, with a corresponding flow volume of ~80–390 km^3. In summary, if the tuff underlying Perseverance was partly consolidated and hydrous, it seems unlikely that the embayment could have formed by thermal erosion unless a series of thinner (<100 m), liquidus or superheated flows incised a reentrant embayment that subsequently become altered by collapse and deformation to its present concave morphology, or a thick (~100 m) superheated flow incised a concave embayment.

Table 3
Model results for the emplacement of 31% MgO Archean komatiite lava flows at Perseverance, W.A

Property (units)	Initially 10-m-thick flow	Initially 30-m-thick flow	Initially 100-m-thick flow
Superheated lavas over wet, welded tuff			
Max. flow distance[a] (km)	30–110	140–480	640–2230
Max. flow thickness[a] (m)	11–15	34–44	110–140
Max. erosion rate[b] (m/day)	20	28	40
Max. erosion depth after 1 week[b] (m)	140	200	270
Max. contamination[a] (%)	10–20	10–20	10–20
Max. crustal thickness[a] (cm)	0.5–4.0	0.3–3.6	0.2–22
Liquidus lavas over unconsolidated tuff			
Max. flow distance[a] (km)	20–70	70–300	300–1250
Max. flow thickness[a] (m)	12–17	37–48	120–150
Max. erosion rate[b] (m/day)	60	82	115
Max. erosion depth after 1 week[b] (m)	420	570	800
Max. contamination[a] (%)	10–20	10–20	10–20
Max. crustal thickness[a] (cm)	3–18	2–15	1–7.8

[a] As turbulent flow.
[b] At vent.

4.5. Case 5: liquidus lava over unconsolidated substrate

Case 5 involves liquidus komatiite flow over a hydrous (50% H_2O), unconsolidated felsic tuff (Fig. 6). Our model results indicate that an initially 100-m-thick komatiite flow will attain contamination of 10–20% at distances of ~380–1660 km from the eruption source due to higher erosion rates (~36–11 m/day). Likewise, an initially 30 m thick komatiite flow will attain these degrees of contamination at distances of ~90–390 km from the eruption source due to erosion rates of ~23–6.4 m/day. An initially 10 m thick komatiite flow will attain these degrees of contamination at distances of ~25–130 km from the eruption source due to erosion rates of ~13–3.1 m/day. For flows of all thicknesses, the vaporization of intergranular sea water fluidizes particles with sizes less than very fine sand (i.e. particle diameters <0.1 mm), thus generating high thermo-mechanical erosion rates and high degrees of contamination (Williams et al., 1998). Although the phenocrysts of the felsic tuff are coarse-sand sized, the ground mass particle size is unknown and we assume that a finer-grained groundmass could have been fluidized by vaporized intergranular sea water, making it easier to remove the remaining material by mechanical erosion. At the erosion rates consistent with the distances given above, only relatively short eruption durations (~7.3–32 days for an initially 10-m-thick flow, ~4.4–16 days for an initially 30-m-thick flow, and ~2.8–9.1 days for an initially 100-m-thick flow) are required to remove 100 m of unconsolidated tuff. These erosion rates and eruption durations correspond to the following flow volumes: 70–280 km^3 for an initially 10 m thick flow; 280–1020 km^3 for an initially 30 m thick flow; and 1230–4010 km^3 for an initially 100 m thick flow. These flow volumes are mostly consistent with the average volumes per flow of the Columbia River flood basalts (5–2093 km^3: Tolan et al., 1989). Thus, our modeling shows that the flowage of liquidus komatiite lavas for tens to hundreds of kilometers over an unconsolidated, water-rich felsic tuff could have produced the highly contaminated flows inferred from geochemical modeling for Perseverance, could have produced the ~100-m-deep Perseverance lava channel by thermo-mechanical erosion within several hundred kilometers of the source, and could have produced large volumes of komatiite lava, consistent with the hypothesis of 'cataclysmic' komatiite flood-like eruptions originally proposed by Barnes et al. (1988a); Hill et al. (1990, 1995).

4.6. Case 6: superheated lava over unconsolidated substrate

If the Perseverance komatiites were superheated

(Fig. 6), then high degrees of contamination (10–20%) would occur still closer to the source due to extended emplacement at higher erosion rates. For an initially 100-m-thick komatiite flow, contamination of ~10–20% is attained at distances of ~220–540 km from the eruption source due to higher erosion rates (~91–56 m/day). Likewise, an initially 30-m-thick komatiite flow will attain these degrees of contamination at distances of ~50–120 km from the eruption source due to erosion rates ~63–35 m/day. An initially 10-m-thick komatiite flow will attain these degrees of contamination at distances of ~15–30 km from the eruption source due to erosion rates of ~42–22 m/day. At these erosion rates, even shorter eruption durations (~2.4–4.6 days for an initially 10-m-thick flow, ~1.6–2.9 days for an initially 30-m-thick flow, and ~1.1–1.8 days for an initially 100-m-thick flow) are required to remove 100 m of unconsolidated tuff. These erosion rates and eruption durations correspond to the following flow volumes: 20–40 km^3 for an initially 10 m thick flow; 100–200 km^3 for an initially 30-m-thick flow; and 510–840 km^3 for an initially 100-m-thick flow. Thus, our modeling shows that the eruption of superheated komatiite flows over an unconsolidated, water-rich felsic tuff could also have produced the highly contaminated Perseverance flows and the ~100-m-deep Perseverance erosional lava channel within tens to hundreds of kilometers of the lava source, and one or more short duration, high volume, komatiite deposits in the Norseman–Wiluna belt (Barnes et al., 1988a; Hill et al., 1990, 1995).

5. Discussion

We again wish to emphasize that the uncertainties and assumptions required to model komatiite lava emplacement and thermal erosion at Perseverance are considerable, and that readers are cautioned to evaluate our results from a practical perspective. From this perspective, we infer from our modeling that Perseverance was most likely formed by a high-volume (flood basalt-sized) eruption of: (1) thinner (10–30 m thick), liquidus or superheated flows that eroded a reentrant lava channel in welded tuff that collapsed to a concave morphology and later filled with lava; or (2) either thin or thick ($\leq$100 m), liquidus or superheated flows that eroded a lava channel in unconsolidated tuff. These results are upheld whether we use a high value of 31% MgO for our initial komatiite composition (Table 3), or a more conservative value of 29% MgO. These results require the formation of long lava channels/tubes (tens to hundreds of kilometers long) and large eruptive volumes (hundreds to a few thousand km^3). It is possible that brecciation of the partly consolidated tuff could have occurred during thermal erosion (such that T_{mg} becomes the effective brecciation temperature, which must lie between the water vaporization temperature and the ground melting temperature). If so, then model results for such a case would lie between those of our unconsolidated tuff model and our partly consolidated tuff model.

There is little preserved field evidence for long komatiite flow conduits in Precambrian greenstone belts, due to the extensive structural deformation of komatiitic terrains. However, Watts and Osmond (2001) recently presented geophysical data of the ultramafic embayments in the Raglan horizon of the Proterozoic Cape Smith Belt of New Québec, which have been interpreted by Green and Dupras (2001) as one or more large, sinuous komatiitic basalt lava channels with a length(s) at least 20 km, perhaps up to 50 km. Although the presence of discrete lava channels is only inferred in some of the Western Australian komatiite sequences, regional mapping suggests that some of these komatiite sequences are continuous over strike distances up to 130 km (e.g. segments of the Norseman–Wiluna Greenstone Belt: Lesher et al., 1984; Barnes et al., 1999; Forrestania Greenstone Belt: Perring et al., 1995). We also note that the longest modern, basaltic lava tube system is that of the Undara Volcano in the McBride Volcanic Province of North Queensland, which is estimated to be ~110 km long (Atkinson et al., 1975), whereas extraterrestrial lava channels and/or tubes are even longer, up to 200–300 km long on Io (Keszthelyi et al., 1999), up to 340 km on the Moon (Schubert et al., 1970) and up to 6800 km on Venus (Head et al., 1991).

The role of thermal erosion in the emplacement of Archean komatiites depends upon many factors, including the composition, viscosity, flow regime, and temperature of the lava, the composition and nature of the substrate, the degree of channelization,

and the environment in which eruption occurs. Thermal erosion by komatiite flows has been inferred in many areas both containing and lacking evidence of lava channelization. However, the best studied localities are those where thermal erosion is associated with lava channels and Fe–Ni–Cu–(PGE) sulfide deposits (Lesher, 1989). There is currently an ongoing debate regarding the emplacement of large lava flow fields, focused primarily on modern flood basalt provinces. Originally, flood basalt lavas were thought to be emplaced turbulently and rapidly (days to weeks), fed by fast channelized flows (Shaw and Swanson, 1970). Recent work suggests some flood basalt flows were emplaced slowly (months to years: Self et al., 1996, 1997), similar to laminarly-flowing, tube-fed, compound, inflationary pahoehoe fields observed in Hawaii (Hon et al., 1994). Similar models have been proposed for Archean komatiites, in which laminar flow and inflation occur at flow fronts (Hill and Perring, 1996; Cas et al., 1999; Dann, 2000). However, these inflationary flow fronts should have been fed by preferred pathways (i.e. lava channels and/or tubes) that could have transported lava rapidly and turbulently. Although inflation could have occurred at Perseverance, our studies show that large scale thermal erosion and inflation are incompatible; lava that vertically inflates a flow is not passing downstream and heating the substrate. If inflation did occur at Perseverance, we believe it likely occurred late in the emplacement of an advancing komatiite flow field, after the establishment of a preferred pathway (i.e. a lava channel or tube) that would have produced a thermal erosion embayment (inflation may well have been ongoing further downstream). Considering the high degree of contamination and depth of the embayment at Perseverance, we believe that large scale thermal erosion in a turbulent, confined flow is required to form such a feature, and that only thermal erosion would have been capable of producing the deep embayment and very highly contaminated lavas at Perseverance.

It is difficult to know the original volume of Archean komatiite sequences such as Perseverance, because of the extent of erosion and deformation in greenstone terrains. Komatiites are a minor component of Archean volcanism (e.g. Viljoen and Viljoen, 1969a,b; de Wit and Ashwal, 1997), and are associated with much more voluminous basaltic and felsic volcanism thought to be associated with Archean mantle plume activity (Campbell et al., 1989). As mantle plumes are also considered to be the source of voluminous continental flood basalts and other large igneous provinces (Mahoney and Coffin, 1997), it seems reasonable that voluminous komatiite flows could have erupted in the Archean. The similarity of our predicted model komatiite flow volumes to the average flow volumes of continental flood basalt flow units (e.g. Tolan et al., 1989) lends support to the idea that voluminous komatiite flows erupted in the Archean. Komatiite eruptions (2.7–3.5 Ga) also roughly coincide with the initiation of voluminous, large impact basin-filling volcanism of rheologically-similar lavas (see Murase and McBirney, 1973; Williams et al., 1999b) on the Moon (3.2–3.9 Ga) and probably the other terrestrial planets as well.

Another result from our modeling of Perseverance is the implication that superheated komatiite lavas may have erupted in the Archean. Although the eruption of superheated lavas has never been observed in modern times, Huppert and Sparks (1985b) suggested that the production of superheated komatiites would require a combination of large flow rates (which appears to be the case for Perseverance) and/or a thin crust (which is likely for the Earth's Archean). Several workers (Lesher and Groves, 1986; Herzberg, 1992; Nisbet et al., 1993) have argued that low-viscosity komatiites would have ascended rapidly, along trajectories with dT/dz closer to an adiabatic path than the liquidus. Other workers have suggested that superheating may have been associated with planetary accretion and the development of magma oceans in hot planetary interiors (e.g. Jakês, 1992), or that superheating can occur in mantle plumes, and may have produced some of the Cretaceous-aged Gorgona Island komatiite lavas (Aitken and Echeverria, 1984; Kerr et al., 1996).

Interesting information from planetary studies relevant to high-temperature lavas comes from recent Galileo spacecraft and telescopic observations of Jupiter's volcanic moon, Io. These data suggest that very high temperature eruptions (~1430–1730°C) are occurring on Io (McEwen et al., 1998), consistent with ultrabasic and/or superheated volcanism (see also Williams et al., 2000). On Io, the source of heat for these high-temperature eruptions is interpreted to be

tidal heating from the gravitational influence of Jupiter (e.g. Yoder and Peale, 1981; Ross and Schubert, 1985). Recently, Greff-Lefftz and Legros (1999) reported modeling results that suggested that solar–lunar tidal forces induced fluid oscillations in Earth's core over geologic time, resulting in resonances that caused periods of high internal friction at the core–mantle boundary, resulting in heat production and mantle plume activity at discreet points in the Earth's past, including ~3.8, ~3.0, ~1.8 Ga, and ~300 Ma. Mantle plumes produced at these first three times may have been responsible for the pulses of komatiitic volcanism at ~3.5 Ga (e.g. Pilbara, Western Australia; Barberton and Belingwe, southern Africa), ~2.7 Ga (e.g. Yilgarn, Western Australia, Barberton, South Africa; Lapland and Kuhmo-Suomussalmi, Finland; Abitibi, Canada; Crixas, South America), and at ~1.8 Ga (Circum-Superior Belt, Canada; Pechenga Belt, Russia). Thus, the relationship between planetary tidal activity and high-temperature volcanism should be further investigated.

6. Summary

We have adapted the komatiite emplacement and erosion model of Williams et al. (1998) to investigate the genesis of the Perseverance embayment in the Norseman–Wiluna greenstone belt of Western Australia. Barnes et al. (1988a, 1995) have proposed that a very voluminous komatiite eruption in the Archean produced a large komatiite 'river' that thermally eroded a 100–150 m deep channel in felsic tuff substrate, resulting in heavily-contaminated (10–20%) lavas and the formation of the Perseverance nickel deposit. We have used constraints from field, modeling, and geochemical studies (Barnes et al., 1988a, 1995; Jarvis, 1995; Libby et al., 1998) to determine under what conditions such highly-contaminated lavas can be produced by surficial thermal erosion. The key results of the modeling may be summarized as follows:

1. It is easier to erode a hydrous, unconsolidated tuff than a hydrous, partly consolidated (welded) tuff than an anhydrous, massive tuff. All else equal, thermal erosion rates and degrees of lava contamination as a function of distance downstream increase for increasingly unconsolidated and water-rich substrates.
2. A superheated lava erupted onto the ocean floor has a greater potential to thermally erode a given substrate than a lava erupted at or below its liquidus temperature, and such lavas will produce higher erosion rates and higher degrees of contamination as a function of distance downstream compared to liquidus lavas.
3. The degree of deformation at Perseverance precludes an exact determination of the morphology of the original lava channel. Either ~100 m thick flow(s) eroded a concave embayment into the felsic tuffaceous substrate, or initially thinner (~10–30 m) flow(s) eroded a large reentrant embayment(s) that subsequently collapsed and/or were altered, resulting in a concave cross-sectional morphology. The most likely scenario from our modeling would have been the emplacement of initially thinner flow(s) of a high (~29% MgO) komatiite that could have thermally eroded the Perseverance embayment if: (a) the lava was either liquidus or superheated and the tuffaceous substrate was water rich and partly consolidated (i.e. welded); or (b) the lava was either liquidus or superheated and the tuffaceous substrate was water rich and unconsolidated. In either case, such flow(s) would attain levels of contamination ~10–20% at distances of tens to hundreds of kilometers from the eruption source. A 100 m deep embayment could have formed in days to weeks, and the corresponding lava volumes are tens to hundreds to thousands of km^3, within the range of values of the average volumes/flow for the Columbia River flood basalts (Tolan et al., 1989).
4. Because our model can produce the observed degree of lava contamination at Perseverance only for unconsolidated or welded tuffaceous substrates, we assume that the substrate was not consolidated.

List of symbols

c_b	lava bulk specific heat, J/kg °C
c_g	substrate specific heat, J/kg °C
c_l	lava liquid specific heat, J/kg °C
c_{vap}	water vapor specific heat, J/kg °C
c_w	sea water specific heat, J/kg °C

d	particle diameter, cm
E_{dg}	energy to disaggregate ground, J/m^3
E_{hg}	energy to heat ground, J/m^3
E_{mg}	energy required to melt substrate, J/m^3
f_L	fraction of heat of fusion to partially melt substrate, J/kg
f_w	fraction of water in substrate
γ	sea water convection parameter, –
g	gravitational acceleration, m/s^2
h	lava flow thickness, m
h_{cs}	steady-state crustal thickness, m
h_T	lava convective heat transfer coefficient, J/m^2 s °C
k_c	lava crust thermal conductivity, J/m s °C
k_{eff}	lava effective thermal conductivity, J/m s °C
k_l	lava thermal conductivity, J/m s °C
k_w	sea water thermal diffusivity,m^2 s
L_g	substrate heat of fusion, J/kg
L_l	lava heat of fusion/crystallization, J/kg
L_{vap}	sea water heat of vaporization, J/kg
λ	lava friction coefficient, –
μ_b	lava bulk dynamic viscosity, Pa s
μ_g	substrate melt dynamic viscosity, Pa s
μ_l	lava liquid dynamic viscosity, Pa s
μ_{vap}	steam dynamic viscosity, Pa s
μ_w	sea water dynamic viscosity, Pa s
ψ	ground slope degrees
Pr	lava Prandtl number, –
ρ_b	lava bulk density, kg/m^3
ρ_c	lava crust density, kg/m^3
ρ_g	substrate density, kg/m^3
ρ_l	lava liquid density, kg/m^3
ρ_{vap}	water vapor density, kg/m^3
ρ_w	sea water density at ambient temperature, kg/m^3
Q_0	initial 2-D flow rate, m^2/s
$Q(x)$	flow rate, m^2/s
Re	lava Reynolds number, –
t	time since flow began, s
T	lava temperature, °C
T_a	ambient temperature of the environment, °C
T_{cs}	steady-state crustal surface temperature, °C
T_{liq}	lava liquidus temperature, °C
T_{mg}	substrate melting temperature, °C
T_{sol}	lava solidus temperature, °C
T_{vap}	sea water vaporization temperature, °C
u	lava flow velocity, m/s
u_m	erosion rate of the substrate, m/s
u_{vap}	steam upflow velocity, m/s
x	distance from source vent, m
X	volume fraction of crystals
$X'(T)$	rate of change of crystal fraction with temperature

Acknowledgements

We are very grateful to Western Mining Corporation for sponsoring our original research on Perseverance. This work represents part of DAW's PhD dissertation, which was funded in part by the National Science Foundation (EAR-9405994) and several University of Alabama Graduate Council Research Fellowships. This manuscript has benefited from two anonymous reviews, as well as many discussions with Steve Self, Rob Hill, and Laszlo Keszthelyi.

Appendix A. Low-viscosity lava emplacement and erosion model

A.1. Flow over dry, consolidated substrates

The following is our base model for low-viscosity, turbulent flow emplacement over anhydrous, consolidates substrates, as described in Williams et al. (1998). Given a set of initial conditions (i.e. lava and substrate major oxide compositions; lava eruption, liquidus, and solidus temperatures; lava flow thickness, ground slope, ground melting temperature, and ambient temperature), our model calculates the initial values of important temperature- and composition-dependent thermal/rheological properties of the lava and substrate (i.e. density, viscosity, specific heat, thermal conductivity, heat of fusion) using algorithms from experimental petrology (Table 1). Auxiliary equations are then used to calculate additional lava properties, including crystallinity (X):

$$X = \frac{T_{liq} - T}{T_{liq} - T_{sol}} \tag{A1}$$

bulk viscosity (μ_b):

$$\mu_b = \mu_l \left(1 - \frac{X}{0.6}\right)^{-2.5} \tag{A2}$$

when $X < 0.3$ and

$$\mu_b = \mu_l \exp\left(\left[2.5 + \left(\frac{X}{0.6 - X}\right)^{0.48}\right]\frac{X}{0.6}\right) \quad \text{(A3)}$$

when $X \geq 0.3$ (Pinkerton and Stevenson, 1992); flow velocity (u), friction coefficient (λ), and Reynolds number (Re) (solved iteratively):

$$u = \sqrt{\frac{4gh\sin(\psi)}{\lambda}} \quad \text{(A4)}$$

$$\lambda = (0.79\ln(\mathrm{Re}) - 1.64)^{-2} \quad \text{(A5)}$$

$$\mathrm{Re} = \frac{\rho_l h u}{\mu_b} \quad \text{(A6)}$$

Prandtl number (Pr):

$$\mathrm{Pr} = \frac{c_l \mu_b}{k_l} \quad \text{(A7)}$$

forced convective heat transfer coefficient (h_T):

$$h_T = \frac{0.027 k_{eff} \mathrm{Re}^{4/5} \mathrm{Pr}^{1/3}}{h}\left(\frac{\mu_b}{\mu_g}\right)^{0.14} \quad \text{(A8)}$$

lava erosion rate (u_m):

$$u_m = \frac{h_T(T - T_{mg})}{E_{mg}} \quad \text{(A9)}$$

and degree of contamination of the lava by assimilated substrate ($S(x)$):

$$S(x) = 1 - \frac{Q_0}{Q(x)}, \qquad Q(x) = Q_0 + \int_0^s u_m \mathrm{d}x \quad \text{(A10)}$$

Lava physical properties (density, specific heat, flow thickness, flow velocity, and heat transfer coefficient) are used to determinate the heat loss from the model flow in a numerical solution of a first-order ordinary differential equation, which gives lava temperature as a function of distance downstream (Huppert and Sparks, 1985a):

$$\rho_b c_l h u \frac{\mathrm{d}T}{\mathrm{d}x} = -h_T(T - T_{mg}) - h_T(T - T_{sol}) - \frac{\rho_b c_l h_T (T - T_{mg})^2}{E_{mg}} + \rho_b c_l h u \frac{\mathrm{d}T}{\mathrm{d}x}\frac{L_l x'(T)}{c_l} \quad \text{(A11)}$$

$$E_{mg} = \rho_g [c_g(T_{mg} - T_a) + f_L L_g] \quad \text{(A12)}$$

In Eq. (A11), we assume that heat loss occurs by forced convection within the turbulent lava to the top and base of the flow, and from thermal erosion that removes the underlying substrate. Heat is gained back from release of latent heat of crystallization.

The steady-state crustal thickness (h_{cs}) at any given distance is calculated assuming a balance between the forced convective heat loss to the top of the lava flow (maintained at the lava solidus, T_{sol}), the conductive heat loss through the growing crust (base at T_{sol}, top at the contact temperature with sea water, T_{cs}), and the natural convective heat loss from the top of the crust to cold sea water:

$$h_{cs} = \frac{k_c(T_{sol} - T_{cs})}{\rho_w c_w \gamma\left(\frac{(\rho_w - \rho_c) g k_w^2}{\mu_w}\right)^{1/3}(T_{cs} - T_a)} \quad \text{(A13)}$$

in which T_{cs} is given by:

$$T_{cs} = T_a + \frac{h_T(T - T_{sol})}{\rho_w c_w \gamma\left(\frac{(\rho_w - \rho_c) g k_w^2}{\mu_w}\right)^{1/3}} \quad \text{(A14)}$$

Since the thermally eroded substrate (S) will be completely assimilated into the turbulently flowing lava (Jellinek and Kerr, 1999), we calculate the compositional change in the liquid lava at each model distance increment using the following mass balance expression:

$$M_{new} = M_{old}(1 - \Delta S) + M_{asm}(\Delta S) \quad \text{(A15)}$$

The compositional change in the liquid lava due to the crystallization of olivine (X) can also be determined using the following mass balance expression:

$$M_{new} = M_{old}(1 - \Delta X) - M_{olv}(\Delta X) \quad \text{(A16)}$$

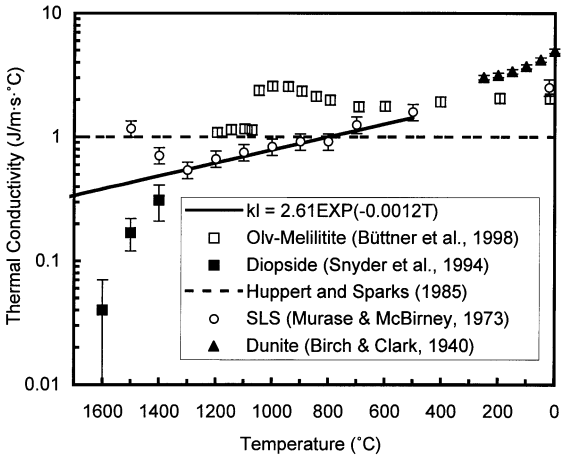

Fig. A1. Graph of lava thermal conductivity (k_l) data (with error bars) as a function of temperature (T), including the curve fitted equation used in our current model. Data are from Büttner et al. (1998: open squares), Snyder et al. (1994: filled squares), Huppert and Sparks (1985a,b: dashed line), Murase and McBirney (1973: synthetic lunar sample (SLS: open circles), and Birch and Clark (1940: filled triangles).

M_{old} in Eq. (A15) is M_{new} from Eq. (A14). Eq. (A15) is used in conjunction with partition coefficient and stoichiometric algorithms to calculate olivine composition at each model increment. Olivine–liquid partition coefficients for Fe^{2+}, Mg, and Ca are from Beattie et al. (1991, 1993); coefficients for Ti and Al are from Kennedy et al. (1993). Eq. (A14) results in a new liquid lava composition that is used to recalculate the temperature- and composition-dependent thermal, rheological, and fluid dynamic properties of the lava at each model increment. Thus, the physical and geochemical evolution of the lava flow with distance is simulated.

A.2. Flow over unconsolidated, water-rich substrates

When the substrate under a turbulent komatiite flow is unconsolidated and water-rich (i.e. a sediment), under certain circumstances particle disaggregation (i.e. mechanical erosion) will occur due to the vaporization of intergranular water. When intergranular water in the substrate is heated by the overlying komatiite, it will rise in temperature to the boiling point (T_{vap}~316°C at a pressure of 100 bars), at which point the water vaporizes. Because water expands as it changes phase from liquid to vapor, this expansion may fragment the unconsolidated substrate, and could enable mechanical mixing with the lava (i.e. mechanical erosion) before subsequent melting in the lava. The energy conservation equation to describe this situation of thermo-mechanical erosion is:

$$\rho_b c_b h u \frac{dT}{dx} = -h_T(T - T_{vap}) - h_T(T - T_{sol}) - \frac{h_T(T - T_{vap})E_{hg}}{E_{dg}} + \rho_l h u \frac{dT}{dx} L_l x'(T) \quad (A17)$$

In this equation, E_{dg} is the energy required to disaggregate the ground (i.e. to heat it up to T_{vap} and then vaporize the water):

$$E_{dg} = (1 - f_w)\rho_g c_g (T_{vap} - T_d) + f_w \rho_w [c_w (T_{vap} - T_a) + L_{vap}] \quad (A18)$$

and E_{hg} is the energy required to heat the disaggregated and mechanically eroded ground up to the lava temperature:

$$E_{hg} = (1 - f_w)\rho_g \left\{ c_g \left(T - T_{vap} \right) + L_g \right\} + f_w \rho_w c_{vap} \left(T - T_{vap} \right) \quad (A19)$$

where f_w is the volume fraction of water in the substrate, L_{vap} is the heat of vaporization of the sea water (J/kg) and c_{vap} is the specific heat of the water vapor (J/kg °C). In the heat transfer coefficient, μ_g is now the viscosity of the fluidized bed, ~1 Pa s (Davidson et al., 1977). The erosion rate u_m is given by:

$$u_m = \frac{h_T(T - T_{vap})}{E_{dg}} \quad (A20)$$

This erosion rate then determines the upflow velocity u_{vap} of steam produced by vaporization of intergranular sea water:

$$u_{vap} = \frac{u_m \rho_w}{\rho_{vap}} \quad (A21)$$

For fluidization of an unconsolidated substrate (Davidson and Harrison, 1963), the steam upflow velocity must be greater than about 1/70 of the settling velocity (u_s) of particles in the water vapor, which depends on the particle density (ρ_p~2600 kg/m^3 for

sediment), the density of steam at depth (~55 kg/m^3), the viscosity of the steam (μ_{vap}~0.00002 Pa s) and the particle diameter (d). Our model predicts that typical steam upflow velocities are ~0.4–0.2 cm/s, which suggests that particles up to the size of very fine sand (<0.1 mm) could have been fluidized in this manner.

Appendix B. Model modifications and reassessment of thermal erosion at Kambalda, Western Australia

We have made two modifications to the numerical model outlined above and in Williams et al. (1998, 1999a). First, the appropriate Reynolds number for describing flow and heat transfer in wide, non-circular full lava tubes (i.e. width $w \gg d$, depth) is given by:

$$\mathrm{Re} = \frac{2\rho_b uh}{\mu_b} \quad \text{(A22)}$$

(e.g. Holman, 1990). This conduit morphology is consistent with that seen at Perseverance, Kambalda, and several other localities. Second, we have used an alternative expression to calculate a temperature-dependent thermal conductivity:

$$k_l = 2.61\exp(-0.0012T) \quad \text{(A23)}$$

see (Fig. A1), because the very low thermal conductivities at high temperatures found by Snyder et al. (1994) may be flawed (Shore, 1995).

Using our updated model, we have also recalculated the thermal erosion produced by high-Mg komatiite lavas at Kambalda. We find that the quantitative results of Williams et al. (1998) are slightly altered, but the qualitative conclusions are unchanged. An initially 10-m-thick, 29% MgO Kambalda komatiite flow over a consolidated anhydrous sediment would produce both the observed surface crustal thickness of 5–20 cm and the measured lava contamination of 2–5% at a distance of 70–200 km downstream from the eruption source, a distance that is consistent with the estimated length of the Kambalda flow field (>45–160 km; see Gresham and Loftus-Hills, 1981; Morris, 1993). At these distances, thermal erosion rates are ~1.2–0.5 m/day, which would have required an eruption duration of ~4–10 days to remove ~5 m of the sulfidic sediment. Thus, it seems likely that the Kambalda komatiites were indeed capable of long distance turbulent flow (tens to hundreds of kilometers), with thermal erosion of the sulfidic sediment as a key factor in the formation of the Kambalda massive sulfide deposits.

References

Aitken, B.G., Echeverria, L.M., 1984. Petrology and geochemistry of komatiites and tholeiites from Gorgona Island, Colombia. Contributions to Mineralogy and Petrology 86, 94–105.

Arndt, N.T., 1976. Melting relations of ultramafic lavas (komatiites) at one atmosphere and high pressure. Carnegie Institute Geophysical Laboratory Yearbook 75, 555–562.

Arndt, N.T., 1986. Thermal erosion by komatiites at Kambalda. Nature 324, 600.

Arndt, N.T., Nisbet, E.G., 1982. Komatiites. George Allen and Unwin, London.

Arndt, N.T., Jenner, G.A., 1986. Crustally contaminated komatiites and basalts from Kambalda, Western Australia. Chemical Geology 56, 229–255.

Arndt, N.T., Naldrett, A.J., Pyke, D.R., 1977. Komatiitic and iron-rich tholeiitic lavas of Munro Township, northeast Ontario. Journal of Petrology 18, 319–369.

Atkinson, A., Griffin, T.J., Stephenson, P.J., 1975. A major lava tube system from Undara volcano, North Queensland. Bulletin of Volcanology 39, 266–293.

Baker, V.R., Komatsu, G., Parker, T.J., Gulick, V.C., Kargel, J.S., Lewis, J.S., 1992. Channels and valleys on Venus: preliminary analysis of Magellan data. Journal of Geophysical Research 97, 13421–13444.

Barnes, S.J., Coates, C.J.A., Naldrett, A.J., 1982. Petrogenesis of a Proterozoic nickel sulfide–komatiite association: the Katiniq Sill, Ungava, Quebec. Economic Geology 77, 413–429.

Barnes, S.J., Hill, R.E.T., Gole, M.J., 1988a. The Perseverance Ultramafic Complex, Western Australia: the product of a komatiite lava river. Journal of Petrology 29, 302–331.

Barnes, S.J., Gole, M.J., Hill, R.E.T., 1988b. The Agnew nickel deposit: Part I. Structure and stratigraphy. Economic Geology 83, 524–536.

Barnes, S.J., Lesher, C.M., Keays, R.R., 1995. Geochemistry of mineralized and barren komatiites from the Perseverance nickel deposit, Western Australia. Lithos 34, 209–234.

Barnes, S.J., Hill, R.E.T., Perring, C.S., Dowling, S.E., 1999. Komatiite flow fields and associated Ni-sulphide mineralisation with examples from the Yilgarn Block, Western Australia. In: Keays, R.R., Lesher, C.M., Lightfoot, P.C., Farrow, C.E.G. (Eds.), Dynamic Processes in Magmatic Ore Deposits and Their Application in Mineral Exploration. Geological Association of Canada Short Course 13, pp. 159–194.

Beattie, P., Ford, C., Russell, D., 1991. Partition coefficients for olivine-melt and orthopyroxene-melt systems. Contributions to Mineralogy and Petrology 109, 212–224.

Beattie, P., Ford, C., Russell, D., 1993. Partition coefficients for

olivine-melt and orthopyroxene-melt systems. Contributions to Mineralogy and Petrology 114, 288.

Birch, F., Clark, H., 1940. The thermal conductivity of rocks and its dependence upon temperature and composition. American Journal of Science, 238, 529–558 and 613–635.

Bottinga, Y., Weill, D.F., 1970. Densities of liquid silicate systems calculated from partial molar volumes of oxide components. American Journal of Science 269, 169–182.

Büttner, R., Zimanowski, B., Blumm, J., Hagemann, L., 1998. Thermal conductivity of a volcanic rock material (olivine–melilitite) in the temperature range between 288 and 1470 K. Journal of Volcanology and Geothermal Research, 80, 293–302.

Campbell, I.H., Griffiths, R.W., Hill, R.I., 1989. Melting in an Archean mantle plume: heads it's basalts, tails it's komatiites. Nature 339, 697–699.

Carr, M.H., 1974. The role of lava erosion in the formation of lunar rilles and Martian channels. Icarus 22, 1–23.

Cas, R., Self, S., Beresford, S., 1999. The behaviour of the fronts of komatiite lavas in medial to distal settings. Earth and Planetary Science Letters 172, 127–139.

Coffin, M.F., Eldholm, O., 1993. Scratching the surface: estimating the dimensions of large igneous provinces. Geology 21, 515–518.

Dann, J.C., 2000. Komatiite flow lobes, inflated sheet flow, and lava tube, 3.5 Ga Komati Formation, Barberton Greenstone Belt, South Africa. Geological Society of America Abstracts w/ Programs 32 (7), A394.

Davidson, J.F., Harrison, D., 1963. Fluidised Particles. Cambridge University Press, London.

Davidson, J.F., Harrison, D., Guedes de Carvalho, J.R.F., 1977. On the liquidlike behavior of fluidized beds. Annual Reviews of Fluid Mechanics 9, 55–86.

Davis, P., Lesher, C.M., McLaughlin, A.D., Clemmer, S., 1993. Komatiite lava channelization, thermal erosion of andesite, and localization of Archean Fe–Ni–Cu sulfide mineralization, Munro Township, Ontario (abstract). Geological Society of America Abstracts w/Programs 25, A400.

de Wit, M., Ashwal, L.D., 1997. Greenstone Belts. Oxford Monographs on Geology and Geophysics 35. Oxford University Press, New York.

Donaldson, C.H., 1982. Spinifex-textured komatiites: a review of textures, mineral compositions and layering. In: Arndt, N.T., Nisbet, E.G. (Eds.), Komatiites. George Allen and Unwin, London.

Evans, D.M., Cowden, A., Barratt, R.M., 1989. Deformation and thermal erosion at the Foster nickel deposit, Kambalda-St Ives, Western Australia. In: Prendergast, M.D., Jones, M.J. (Eds), Magmatic Sulphides—The Zimbabwe Volume. London, Institution of Mining and Metallurgy, pp. 215–219.

Fritz, W.J., Stillman, C.J., 1996. A subaqueous welded tuff from the Ordovician of County Waterford, Ireland. Journal of Volcanology and Geothermal Research 70, 91–106.

Frost, K.M., Groves, D.I., 1989. Ocellar units at Kambalda: evidence for sediment assimilation by komatiite lavas. In: Prendergast, M.D., Jones, M.J. (Eds.), Magmatic Sulphides—The Zimbabwe Volume. London, Institution of Mining and Metallurgy, pp. 207–213.

Gee, R.D., Baxter, J.L., Wilde, S.A., Williams, I.R., 1981. Crustal development in the Archean Yilgarn Block, Western Australia, Geological Society of Australia Special Paper 7, pp. 43–56.

Ghiorso, M.S., Sack, R.O., 1995. Chemical mass transfer in magmatic processes IV. A revised and internally consistent thermodynamic model for the interpolation and extrapolation of liquid–solid equilibria in magmatic systems at elevated temperatures and pressures. Contributions to Mineralogy and Petrology 119, 197–212.

Gillies, S.L., Lesher, C.M., 1992. Lava channelization in the Katiniq Peridotite Complex, Cape Smith Belt, New Québec (abstract). Geological Society of America Abstracts w/Programs 24, A267.

Gole, M.J., Barnes, S.J., Hill, R.E.T., 1987. The role of fluids in the metamorphism of komatiites, Agnew nickel deposit, Western Australia. Contributions to Mineralogy and Petrology 96, 151–162.

Greeley, R., Fagents, S.A., Harris, R.S., Kadel, S.D., Williams, D.A., Guest, J.E., 1998. Evidence for erosion by flowing lava and planetary implications. Journal of Geophysical Research 103, 27325–27346.

Green, A.H., Dupras, N., 2001. Exploration model for komatiitic peridotite-hosted Ni–Cu–(PGE) mineralization in the Raglan Belt. In: Lesher, C.M. (Ed.), Magmatic Fe–Ni–Cu–(PGE Deposits in the Cape Smith Belt, New Quebec. Society of Economic Geologists, Special Publication, submitted.

Gresham, J.J., Loftus-Hills, G.D., 1981. The geology of the Kambalda nickel field, Western Australia. Economic Geology 76, 1373–1416.

Greff-Lefftz, M., Legros, H., 1999. Core rotational dynamics and geological events. Science 286, 1707–1709.

Groves, D.I., Korkiakoski, E.A., McNaughton, N.J., Lesher, C.M., Cowden, A., 1986. Thermal erosion by komatiites at Kambalda, Western Australia and the genesis of nickel ores. Nature 319, 136–139.

Head, J.W., Campbell, D.B., Elachi, C., Guest, J.E., McKenzie, D.P., Saunders, R.S., Schaber, G.G., Schubert, G., 1991. Venus volcanism: initial analysis from Magellan data. Science 252, 276–288.

Herzberg, C., 1992. Depth and degree of melting of komatiites. Journal of Geophysical Research 97, 4521–4540.

Hill, R.E.T., Barnes, S.J., Gole, M.J., Dowling, S.E., 1990. Physical Volcanology of Komatiites, Excursion Guidebook #1, Geological Society of Australia (Western Australia Division), Perth.

Hill, R.E.T., Barnes, S.J., Gole, M.J., Dowling, S.E., 1995. The volcanology of komatiites as deduced from field relationships in the Norseman–Wiluna greenstone belt, Western Australia. Lithos 34, 159–188.

Hill, R.E.T., Perring, C.S., 1996. The evolution of Archean komatiite flow fields—are they inflationary sheet flows? AGU Chapman Conference on Long Lava Flows Conference Abstracts, Whitehead, P.W. (Ed.), Economic Geology Research Unit Contribution 56, James Cook University of North Queensland, pp. 18–21.

Holman, J.P., 1990. Heat Transfer. 7th edMcGraw-Hill, New York.

Hon, K., Kauahikaua, J., Delinger, R., Mackay, K., 1994. Emplacement and inflation of pahoehoe sheet flows: observations and

measurements of active lava flows on Kilauea Volcano, Hawaii. Geological Society of America Bulletin 106, 351–370.

Hulme, G., 1973. Turbulent lava flows and the formation of lunar sinuous rilles. Modern Geology 4, 107–117.

Huppert, H.E., 1989. Phase changes following the initiation of a hot turbulent flow over a cold solid substrate. Journal of Fluid Mechanics 198, 293–319.

Huppert, H.E., Sparks, R.S.J., Turner, J.S., Arndt, N.T., 1984. Emplacement and cooling of komatiite layers. Nature 309, 19–22.

Huppert, H.E., Sparks, R.S.J., 1985a. Komatiites I: eruption and flow. Journal of Petrology 26, 694–725.

Huppert, H.E., Sparks, R.S.J., 1985b. Cooling and contamination of mafic and ultramafic magmas during ascent through continental crust. Earth and Planetary Science Letters 74, 371–386.

Jakês, P., 1992. Superheat in magma oceans. In: Agee, C.B., Longhi, J. (Eds.), Workshop on the Physics and Chemistry of Magma Oceans from 1 bar to 4 mbar. LPI Tech. Rep. 92-03, Lunar and Planetary Institute, Houston, pp. 26–27.

Jarvis, R.A., 1995. On the cross-sectional geometry of thermal erosion channels formed by turbulent lava flows. Journal of Geophysical Research 100, 10127–10140.

Jellinek, A.M., Kerr, R.C., 1999. Mixing and compositional stratification produced by natural convection. 2. Applications to the differentiation of basaltic and silicic magma chambers and komatiite lava flows. Journal of Geophysical Research 104, 7203–7218.

Kauahikaua, J., Cashman, K., Hon, K., Mattox, T.N., Heliker, C., Mangan, M., Thornber, C., 1998. Observations on basaltic lava streams in tubes from Kilauea Volcano, Hawaii. Journal of Geophysical Research 103, 27303–27323.

Kennedy, A.K., Lofgren, G.B., Wasserburg, G.J., 1993. An experimental study of trace element partitioning between olivine, orthopyroxene, and melt in chrondrules: equilibrium values and kinetic effects. Earth and Planetary Science Letters 115, 177–195.

Kerr, A.C., Marriner, G.F., Arndt, N.T., Tarney, J., Nivia, A., Saunders, A.D., Duncan, R.A., 1996. The petrogenesis of Gorgona komatiites, picrites and basalts: new field, petrographic and geochemical constraints. Lithos 37, 245–260.

Kerr, R.C., 2001. Thermal erosion by laminar lava flows. Journal of Geophysical Research (submitted).

Keszthelyi, L., Self, S., 1998. Some physical requirements for the emplacement of long basaltic lava flows. Journal of Geophysical Research 103, 27447–27464.

Keszthelyi, L., McEwen, A., Davies, A., Smythe, W., Williams, D., the Galileo SSI and NIMS Teams, 1999. Do we believe the extreme temperatures for Io volcanism and what does it tell us? Eos 80, F624.

Kokelaar, B.P., 1982. Fluidization of wet sediments during the emplacement and cooling of various igneous bodies. J. Geol. Soc. London 139, 21–33.

Kokelaar, P., Busby, C., 1992. Subaqueous explosive eruption and welding of pyroclastic deposits. Science 257, 196–201.

Lange, R.A., Navrotsky, A., 1992. Heat capacities of Fe_2O_3-bearing silicate liquids. Contributions to Mineralogy and Petrology 110, 311–320.

Lesher, C.M., 1983. Localization and genesis of komatiite-associated Fe–Ni–Cu sulphide mineralization at Kambalda, Western Australia, PhD dissertation. University of Western Australia, Nedlands.

Lesher, C.M., 1989. Komatiite-associated nickel sulfide deposits. In: Whitney, J.A., Naldrett, A.J. (Eds.), Ore deposits associated with magmas. Reviews in Economic Geology 4, 45–102.

Lesher, C.M., Groves, D.I., 1986. Controls on the formation of komatiite-associated nickel–copper sulfide deposits. In: Friedrich, G.H., Genkin, A.D., Naldrett, A.J., Ridge, J.D., Sillitoe, R.H., Vokes, F.M. (Eds.), Geology and Metallogeny of Copper Deposits. Springer-Verlag, Berlin, pp. 43–62.

Lesher, C.M., Campbell, I.H., 1993. Geochemical and fluid dynamic modeling of compositional variations in Archean komatiite-hosted nickel sulfide ores in Western Australia. Economic Geology 88, 804–816.

Lesher, C.M., Arndt, N.T., 1995. REE and Nd geochemistry, petrogenesis, and volcanic evolution of contaminated komatiites at Kambalda, Western Australia. Lithos 34, 127–158.

Lesher, C.M., Stone, W.E., 1996. Exploration geochemistry of komatiites. In: Wyman, D.A. (Ed.), Igneous Trace Element Geochemistry Applications for Massive Sulfide Exploration. GAC-MAC Short Course Notes 12, 153–204.

Lesher, C.M., Thibert, F., Mallinson, T., 2001a. Stratigraphy and physical volcanology of komatiitic peridotite lava channels, channelized sheet flows, and channelized sheet sills in the Cape Smith Belt, New Quebec. In: Lesher, C.M. (Ed.), Magmatic Fe–Ni–Cu–(PGE) Deposits in the Cape Smith Belt, New Quebec. Society of Economic Geologists, Special Publication, in review.

Lesher, C.M., Arndt, N.T., Groves, D.I., 1984. Genesis of komatiite-associated nickel sulphide deposits at Kambalda, Western Australia: a distal volcanic model. In: Buchanan, D.L., Jones, M.J. (Eds.), Sulphide Deposits in Mafic and Ultramafic Rocks. Institute of Mining and Metallurgy, London, pp. 70–80.

Lesher, C.M., Burnham, O.M., Keays, R.R., Barnes, S.J., Hulbert, L., 1999. Geochemical discrimination of barren and mineralised komatiites in dynamic ore-forming magmatic systems. In: Keays, R.R., Lesher, C.M., Lightfoot, P.C., Farrow, C.E.G. (Eds.), Dynamic Processes in Magmatic Ore Deposits and Their Application in Mineral Exploration. Geological Association of Canada Short Course 13, pp. 451–477.

Lesher, C.M., Burnham, O.M., Keays, R.R., Barnes, S.J., Hulbert, L., 2001b. Geochemical discrimination of barren and mineralised komatiites associated with magmatic Ni-Cu-(PGE) sulphide deposits. Canadian Mineralogist (accepted).

Libby, J.W., Stockman, P.R., Cervoj, K.M., Muir, M.R.K., Whittle, M., Langworthy, P.J., 1998. Perseverance nickel deposit. In: Mackenzie, D.H., Berkman, D.A. (Eds.), Geology of Australian and Papua New Guinean Mineral Deposits. The Australasian Institute of Mining and Metallurgy, Melbourne, Australia, pp. 321–328.

Mahoney, J.J., 1987. An isotopic survey of Pacific oceanic plateaus: implications for their nature origin. In: Keating. B., Fryer, P., Batiza, B., Boehlert, G. (Eds.), Seamounts, Islands, and Atolls, Geophysical Monographs Series 43. AGU, Washington, DC, pp. 207–220.

Mahoney, J.J., Coffin, M.F., 1997. Large Igneous Provinces: Continental, Oceanic, and Planetary Flood Volcanism. AGU Geophysical Monograph 100. American Geophysical Union, Washington, DC.

McEwen, A.S., Keszthelyi, L., Spencer, J.R., Schubert, G., Matson, D.L., Lopes-Gautier, R., Klaasen, K.P., Johnson, T.V., Head, J.W., Geissler, P., Fagents, S., Davies, A.G., Carr, M.H., Breneman, H.H., Belton, M.J.S., 1998. High-temperature silicate volcanism on Jupiter's moon Io. Science 281, 87–90.

McNaughton, N.J., Frost, K.M., Groves, D.I., 1988. Ground melting and ocellar komatiites: a lead isotopic study at Kambalda, Western Australia. Geological Magazine 125, 285–295.

Mo, X., Carmichael, I.S.E., Rivers, M., Stebbins, J., 1982. The partial molar volume of Fe_2O_3 in multicomponent silicate liquids and the pressure dependence of oxygen fugacity in magmas. Mineralogical Magazine 45, 237–245.

Morris, P., 1993. Physical volcanology and geochemistry of Archean mafic and ultramafic volcanic rocks between Menzies and Norseman, Eastern Yilgarn Craton, Western Australia, Report 36, Geological Society of Western Australia, Perth.

Murase, T., McBirney, A.R., 1973. Properties of some common igneous rocks and their melts at high temperatures. Geological Society of America Bulletin 84, 3563–3592.

Myers, J.S., 1988. Precambrian, in Geology and Mineral Resources of Western Australia. Western Australia Geological Survey Memoir 3, 737–750.

Naldrett, A.J., 1989. Magmatic Sulphide Deposits. Oxford University Press, New York.

Navrotsky, A., 1995. Energetics of silicate melts. In: Stebbins, J.F., McMillan, P.F., Dingwell, D.B. (Eds.), Structure, Dynamics and Properties of Silicate Melts. Reviews in Mineralogy 32, 121–142.

Nisbet, E.G., 1982. The tectonic setting and petrogenesis of komatiites. In: Arndt, N.T., Nisbet, E.G. (Eds.), Komatiites. Allen and Unwin, Winchester, MA, pp. 501–520.

Nisbet, E.G., Cheadle, M.J., Arndt, N.T., Bickle, M.J., 1993. Constraining the potential temperature of the Archean mantle: a review of the evidence from komatiites. Lithos 30, 291–307.

Perring, C.S., Barnes, S.J., Hill, R.E.T., 1995. The physical volcanology of Archean komatiite sequences from Forrestania, Southern Cross Province, Western Australia. Lithos 34, 189–208.

Peterson, D.W., Holcomb, R.T., Tilling, R.I., Christiansen, R.L., 1994. Development of lava tubes in the light of observations at Mauna Ulu, Kilauea Volcano, Hawaii. Bulletin of Volcanology 56, 343–360.

Pinkerton, H., Stevenson, R.J., 1992. Methods of determining the rheological properties of magmas at sub-liquidus temperatures. Journal of Volcanology and Geothermal Research 53, 47–66.

Ross, J.R., Hopkins, G.M.F., 1975. Kambalda nickel sulphide deposits. In: Knight, C.L. (Ed.), Economic Geology of Australia and Papua New Guinea, I: Metals, Monograph 5. Australasia Institute of Mining and Metallurgy, Carlton South, Victoria, pp. 100–121.

Ross, M.N., Schubert, G., 1985. Tidally forced viscous heating in a partially molten Io. Icarus 64, 391–400.

Ryan, M.P., Sammis, C.G., 1981. The glass transition in basalt. Journal of Geophysical Research 86, 9516–9539.

Schmincke, H.-U., Weaver, P.P.E., Firth, J.V., Baraza, J., Bristow, J.F., Brunner, C., Carey, S., Coakley, B., Fuller, M., Funck, T., Gerard, M., Goldstrand, P., Herr, B., Hood, J., Howe, R., Jarvis, I., Lebreiro, S., Lindblom, S., Lykke-Andersen, H., Maniscalco, R., Rothwell, G., Sblendorio-Levy, J., Schneider, J.-L., Sumita, M., Tanguchi, H., Tu, P., Wallace, P., 1995. Proceedings of the Ocean Drilling Program, Initial Reports, vol. 157, College Station, Texas, Ocean Drilling Program.

Schubert, G., Lingenfelter, R.E., Peale, S.J., 1970. The morphology, distribution, and origin of lunar sinuous rilles. Reviews of Geophysics and Space Physics 8, 199–225.

Self, S., Thordarson, T., Keszthelyi, L., Walker, G.P.L., Hon, K., Murphy, M.T., Long, P., Finnemore, S., 1996. A new model for the emplacement of Columbia River basalts as large, inflated pahoehoe lava flow fields. Geophysical Research Letters 23, 2689–2692.

Self, S., Thordarson, T., Keszthelyi, L., 1997. Emplacement of continental flood basalt lava flows. In: Mahoney, J.J., Coffin, M. (Eds.), AGU Monograph on Large Igneous Provinces. American Geophysical Union, pp. 381–410.

Shaw, H.R., 1972. Viscosities of magmatic silicate liquids: an empirical method of prediction. American Journal of Science 272, 870–893.

Shaw, H.R., Swanson, D.A., 1970. Eruption and flow rates of flood basalts. In: Gilmour, E.H., Stradling, D. (Eds.), Proceedings of the Second Columbia River Basalt Symposium, Cheney. Eastern Washington State College Press, pp. 270–299.

Shore, M., 1995. Comment on 'Experimental determination of th thermal conductivity of molten $CaMgSi_2O_6$ and the transport of heat through magmas' by Don Snyder, Elizabeth Gier, and Ian Carmichael. Journal of Geophysical Research 100, 22401–22402.

Snyder, D., Gier, E., Carmichael, I., 1994. Experimental determination of the thermal conductivity of molten $CaMgSi_2O_6$ and the transport of heat through magmas. Journal of Geophysical Research 99, 15503–15516.

Sparks, R.S.J., Sigurdsson, H., Carey, S.N., 1980. The entrance of pyroclastic flows into the sea. II. Theoretical considerations on subaqueous emplacement and welding. Journal of Volcanology and Geothermal Research 7, 97–105.

Swanson, D.A., 1975. Pahoehoe flows from the 1969–71 Mauna Ulu eruption, Kilauea Volcano, Hawaii. Bulletin of the Geological Society of America 84, 615–626.

Tolan, T., Reidel, S.P., Beeson, M.H., Anderson, J.L., Fecht, K.R., Swanson, D.A., 1989. Revisions to the estimates of the areal extent and volume of the Columbia River Basalt Group. In: Reidel, S.P., Hooper, P.R. (Eds.), Volcanism and Tectonism in the Columbia River Flood-Basalt Province. Geological Society of America Special Paper 239, pp. 1–20.

Viljoen, M.J., Viljoen, R.P., 1969a. Evidence for the existence of a mobile extrusive peridotic magma from the Komati Formation of the Onverwacht Group. Special Publication of the Geological Society of South Africa 2, 87–112.

Viljoen, M.J., Viljoen, R.P., 1969b. The geology and geochemistry of the lower ultramafic unit of the Onverwacht Group and a

proposed new class of igneous rock. Special Publication of the Geological Society of South Africa 2, 55–85.

Walker, D., Kirkpatrick, R.J., Longhi, J., Hays, J.F., 1976. Crystallization history of lunar picritic basalt sample 12002: phase-equilibria and cooling-rate studies. Geological Society of America Bulletin 87, 646–656.

Watts, T., Osmond, R., 2001. 3D geophysical model of the Raglan Belt. In: Lesher, C.M. (Ed.), Magmatic Fe–Ni–Cu–(PGE) Deposits in the Cape Smith Belt, New Quebec. Society of Economic Geologists, Special Publication, submitted.

Westrich, H.R., Stockman, H.W., Eichelberger, J.C., 1988. Degassing of rhyolitic magma during ascent and emplacement. Journal of Geophysical Research 93, 6503–6511.

Williams, D.A., Kerr, R.C., Lesher, C.M., 1998. Emplacement and erosion by Archean komatiite lava flows at Kambalda: revisited. Journal of Geophysical Research 103, 27533–27549.

Williams, D.A., Kerr, R.C., Lesher, C.M., 1999a. Thermal and fluid dynamics of komatiitic lavas associated with magmatic Fe–Ni–Cu–(PGE) sulphide deposits. In: Keays, R.R., Lesher, C.M., Lightfoot, P.C., Farrow, C.E.G. (Eds.), Dynamic Processes in Magmatic Ore Deposits and Their Application in Mineral Exploration. Geological Association of Canada Short Course 13, pp. 367–412.

Williams, D.A., Lesher, C.M., Kerr, R.C., 1999b. Komatiitic lava channels in the Cape Smith Belt, New Québec: analogs to the lunar sinuous rilles? Geological Society of America Abstracts w/Programs 31, A263.

Williams, D.A., Wilson, A.H., Greeley, R., 2000. A komatiite analog to potential ultramafic materials on Io. Journal of Geophysical Research 105, 1671–1684.

Yoder, C.F., Peale, S.J., 1981. The tides of Io. Icarus 47, 1–35.